

AD-A164 688

AN ISOSTATIC EARTH MODEL (U) OHIO STATE UNIV COLUMBUS
DEPT OF GEODETIC SCIENCE AND SURVEYING H SUENKEL
SEP 85 OSU/DBSS-367 AFGL-TR-85-8239 F19628-82-K-0017

1/1

UNCLASSIFIED

F/G 8/5

NL

					END								
					mtd								
					4								
					otic								



MICROCOPY RESOLUTION TEST CHART
NATIONAL BUREAU OF STANDARDS-1963-A

12

AFGL-TR-85-0239

AN ISOSTATIC EARTH MODEL

AD-A164 608

DTIC
SELECTE
FEB 21 1986
S D D

HANS SÜNKEL

DEPARTMENT OF GEODETIC SCIENCE AND SURVEYING
THE OHIO STATE UNIVERSITY
COLUMBUS, OHIO

SEPTEMBER 1985

SCIENTIFIC REPORT NO. 10

APPROVED FOR PUBLIC RELEASE: DISTRIBUTION UNLIMITED

AIR FORCE GEOPHYSICS LABORATORY
AIR FORCE SYSTEMS COMMAND
UNITED STATES AIR FORCE
HANSCOM AFB, MASSACHUSETTS 01731

DTIC FILE COPY

86 2 21 081

CONTRACTOR REPORTS

This technical report has been reviewed and is approved for publication.


CHRISTOPHER JEKELY
Contract Manager


THOMAS P. ROONEY
Chief, Geodesy & Gravity Branch

FOR THE COMMANDER


DONALD H. ECKHARDT
Director
Earth Sciences Division

This report has been reviewed by the ESD Public Affairs Office (PA) and is releasable to the National Technical Information Service (NTIS).

Qualified requestors may obtain additional copies from the Defense Technical Information Center. All others should apply to the National Technical Information Service.

If your address has changed, or if you wish to be removed from the mailing list, or if the addressee is no longer employed by your organization, please notify AFGL/DAA, Hanscom AFB, MA 01731. This will assist us in maintaining a current mailing list.

REPORT DOCUMENTATION PAGE		READ INSTRUCTIONS BEFORE COMPLETING FORM
1. REPORT NUMBER AFGL-TR-85-0239	2. GOVT ACCESSION NO. AD A164608	3. RECIPIENT'S CATALOG NUMBER
4. TITLE (and Subtitle) AN ISOSTATIC EARTH MODEL	5. TYPE OF REPORT & PERIOD COVERED Scientific Report No. 10	
	6. PERFORMING ORG. REPORT NUMBER Report N. 367	
7. AUTHOR(s) Hans Sünkel	8. CONTRACT OR GRANT NUMBER(s) F-19628-82-K-0017	
9. PERFORMING ORGANIZATION NAME AND ADDRESS Department of Geodetic Science and Surveying The Ohio State University Columbus, Ohio, 43210	10. PROGRAM ELEMENT, PROJECT, TASK AREA & WORK UNIT NUMBERS 62101F 760003AM	
11. CONTROLLING OFFICE NAME AND ADDRESS Air Force Geophysics Laboratory Hanscom AFB, Mass.01731 Contract Monitor - Christopher Jekeli/LWG	12. REPORT DATE September 1985	
	13. NUMBER OF PAGES 58	
14. MONITORING AGENCY NAME & ADDRESS (if different from Controlling Office)	15. SECURITY CLASS. (of this report) Unclassified	
	15a. DECLASSIFICATION/DOWNGRADING SCHEDULE Unclassified	
16. DISTRIBUTION STATEMENT (of this Report) Approved for public release; distribution unlimited		
17. DISTRIBUTION STATEMENT (of the abstract entered in Block 20, if different from Report)		
18. SUPPLEMENTARY NOTES		
19. KEY WORDS (Continue on reverse side if necessary and identify by block number) isostasy, topographic-isostatic potential harmonic analysis and synthesis; fast Fourier transform; smoothing operators; <i>Operators (Mathematics)</i> .		
20. ABSTRACT (Continue on reverse side if necessary and identify by block number) The concept of the conventional Airy/Heiskanen isostatic model is investigated from scratch, based on the harmonic analysis of the topographic-isostatic potential. First and higher order approximations for those coefficients are discussed and rule of thumb formulas given. The estimated frequency transfer function between the power spectrum of the observed gravitational field and the power spectrum implied by the isostatic model strongly suggests a smoothing of the compensation surface according to		

20. (cont)

Vening Meinesz with a smoothing operator of Gaussian bell-shaped type, and a depth of compensation of about 24 km. A proof of equivalence of using a standard Airy/Heiskanen model with a larger compensation depth and a corresponding Poisson smoothed Vening Meinesz model at a smaller depth has been given for the case of linear approximation, yielding an entirely new interpretation of recently discussed isostatic models.

An iterative least-squares process has been designed which provided parameter estimates of that isostatic model in best possible agreement with the observed gravitational potential of the earth. Based on these parameters, a set of harmonic coefficients of the topographic-isostatic potential, complete up to degree and order 180, has been computed. Several maps of topography-isostasy implied geoidal heights are presented for comparison and illustration purposes.

Both the complete set of harmonic coefficients and the used program source code may be requested from the author.

FOREWORD

This report was prepared by Dr. Hans Sünkel, Professor, Technical University at Graz, Austria, under Air Force Contract No. F19628-79-K-0017, The Ohio State University Research Foundation, Project No. 714255, Project Supervisor, Dr. Urho A. Uotila, Professor, Department of Geodetic Science and Surveying. The contract covering this research is administered by the Air Force Geophysics Laboratory (AFGL), Hanscom Air Force Base, Massachusetts, with Dr. Christopher Jekeli, Contract Monitor.

Accession For	
NTIS CRA&I	<input checked="" type="checkbox"/>
DTIC TAB	<input type="checkbox"/>
Unannounced	<input type="checkbox"/>
Justification	
By	
Distribution /	
Availability Codes	
Dist	Avail and/or Special
A-1	

CONTENTS

1.	Introduction	1
2.	Harmonic Analysis of the Topographic-Isostatic Potential	3
3.	Approximations for the Harmonic Coefficients of the Topographic-Isostatic Potential	8
3.1	Linear Approximation	8
3.2	Higher Order Approximations	10
3.3	The Second Order Effect	11
4.	Power Spectrum Considerations	15
4.1	Compensation Depth vs. Smoothing	17
5.	An Optimal Vening Meinesz Isostatic Model	22
5.1	Estimation of the Parameters of the Smoothing Operator	22
5.2	Fine-Tuning of Parameter Estimation	25
6.	Numerical Studies, Results, Conclusions	28
	Acknowledgements	51
	References	52

1. INTRODUCTION

The theory of isostasy has a well-documented history of more than a hundred years. Its fundamentals are even considerably older and can be traced back to Archimedes. From geodetic evidences some kind of isostatic equilibrium had to be postulated. Although in some limited areas the Pratt/Hayford system seemed to prevail, the Airy/Heiskanen system is now generally believed to model the complex reality better.

The geodetic interest in isostasy was considerably fueled both by the access to high speed computers and the release of a worldwide digital terrain model. Harmonic coefficients of the topographic-isostatic potential have been calculated by several colleagues up to degree and order 36, based on $5^\circ \times 5^\circ$ mean topographic information, both in linear approximation (Khan, 1973) and in the non-linear mode (Lachapelle, 1975). At that time much higher resolutions could not be obtained because of missing data, but in particular because of excessive computer time requirements. With the design of the fast Fourier algorithm on the sphere by Colombo (1981) and the public release of his programs, high resolution models became suddenly feasible and have been computed complete up to degree 180 by Rapp (1982a) based on the worldwide digital topographic model of 64800 $1^\circ \times 1^\circ$ mean elevations provided by DMAAC in 1979 and using the Airy/Heiskanen model in linear approximation. Rapp claimed that correlation studies between his geopotential solution of 1981 and the topographic-isostatic potential suggest a considerably deeper level of compensation of about 50 km rather than the usually used value of 30 km. Rapp's linear approximation has been extended recently, taking into account also second and third order terms, by Rummel (private communication). For a compensation depth of 50 km the agreement between the topography-isostasy and the geopotential spectrum was very good in the frequency range between degree 50 and 150; however, rather poor results have been obtained for the range between degree 20 and 50 and, what is more astonishing, also in the high frequency range above 150.

In 1983 an "exact" solution has been produced by former colleagues at the Technical University in Graz using the same DMAAC data set, but

unfortunately a less exact computer program which yielded, softly speaking, not utterly reliable results. Since this data set is often identified with my name for unidentified reasons, I feel obliged to clarify: it is not my product.

Tscherning (1984) compared existing solutions, found that the above referenced data set must be in doubt, criticized Rapp's 1982 solution because of the too large and therefore, hard to sell depth of compensation, and suggested the use of much smaller compensation depths in the range between 15 and 35 km which he found "optimal" in terms of maximally reducing the power of the observed geopotential.

The question of the meat between the sandwich triggered my interest and was a challenge to investigate that problem from scratch. The goal of this study was to estimate the parameter(s) of the most likely compensation model which is in best possible agreement with the observed geopotential and also geophysically acceptable, and the calculation of the harmonic coefficients of the topographic-isostatic potential complete up to degree and order 180, based on that model.

Now you may continue with Chapter 6, the other part of the sandwich, and if you are turned on, you may even find some meat between.

2. HARMONIC ANALYSIS OF THE TOPOGRAPHIC-ISOSTATIC POTENTIAL

The topographic-isostatic potential of Airy/Heiskanen type T_{II} is defined as the potential of all mass disturbances relative to an ideal crustal layer of uniform density ρ_0 and thickness D , superimposed upon underlying material of equally uniform density, ρ_1 . Denoting the mass disturbance by $\delta\rho$, the potential T_{II} is well-known to be given by

$$T_{II}(P) = G \iiint_V s^{-1}(P,Q) \delta\rho(Q) dv(Q) \quad (2-1)$$

with G ... Newton's gravitational constant,
 $s(P,Q)$... space distance between P and Q ,
 dv ... volume element.

T_{II} is certainly harmonic outside the earth's surface and T_{II} 's spherical harmonic series is certainly convergent outside a sphere completely enclosing the earth. Outside that sphere we may use the convergent series representation of s^{-1} ,

$$s^{-1}(P,Q) = \sum_{n=0}^{\infty} \frac{r_Q^n}{r_P^{n+1}} P_n(\cos \psi_{PQ}) \quad (2-2)$$

with r ... modulus of the radius vector,
 ψ_{PQ} ... spherical distance between P and Q ,
 P_n ... Legendre polynomial of degree n

(Heiskanen & Moritz, 1967 (HM), p. 33). Decomposing P_n in terms of

$$P_n(\cos \psi_{PQ}) = \frac{1}{2n+1} \sum_{m=-n}^n \bar{R}_{nm}(P) \bar{R}_{nm}(Q) \quad (2-3)$$

with the fully normalized spherical harmonics \bar{R}_{nm} ,

$$\bar{R}_{nm}(P) = \sqrt{2^{1-\delta_{m0}}(2n+1) \frac{(n-m)!}{(n+m)!}} P_{nm}(\cos \theta_p) \begin{cases} \cos m \lambda_p & \text{for } m < 0 \\ \sin m \lambda_p & \text{for } m > 0 \end{cases} \quad (2-4)$$

(δ_{ij} ... Kronecker symbol, P_{nm} ... Legendre function, θ , λ ... polar distance, longitude.), the topographic-isostatic potential is represented by the harmonic

series

$$T_{II}(P) = G \sum_{n=0}^{\infty} r_p^{-(n+1)} \frac{1}{2n+1} \sum_{m=-n}^n \bar{R}_{nm}(P) \iiint_V \delta\rho(Q) r^n(Q) \bar{R}_{nm}(Q) dv(Q) \quad (2-5)$$

with $dv(Q) = r^2(Q) dr(Q) d\sigma(Q)$

and the spherical surface element $d\sigma$.

Let us now investigate the volume integral, confining ourselves to the usual spherical approximation. Then its contribution due to the topographical masses outside the geoid and ocean water inside the geoid is

$$\iint_{\sigma} \int_{r=R}^{R+H} \delta\rho(Q) r^{n+2}(Q) dr(Q) \bar{R}_{nm}(Q) d\sigma(Q), \quad (2-6a)$$

and its contribution due to the isostatically compensating masses is

$$\iint_{\sigma} \int_{r=R-D+kH}^{R-D} \delta\rho(Q) r^{n+2}(Q) dr(Q) \bar{R}_{nm}(Q) d\sigma(Q), \quad (2-6b)$$

with R . . . mean earth radius,

D . . . depth of compensation level,

H . . . topographical height (+),
ocean bottom height (-),

k . . . compensation "factor".

(The compensation "factor" k , which is in the non-planar case actually a function slightly dependent on H , will be discussed later.) In (2-6a) the function

$\delta\rho = \rho_0 = \text{constant for topographic masses,}$

$\delta\rho = \rho_w - \rho_0 = \text{constant for ocean masses,}$

in (2-6b)

$\delta\rho = \rho_0 - \rho_1 = \text{constant for compensating masses}$

is used ($\rho_w = \text{density of ocean water}$). The integration of (2-6a,b) with

respect to r is straightforward and yields

$$\frac{R^{n+3}}{n+3} \iint_{\sigma} \delta\rho(Q) \left[\left(1 + \frac{H(Q)}{R} \right)^{n+3} - 1 \right] \bar{R}_{nm}(Q) d\sigma(Q) \quad (2-6a)'$$

and

$$\frac{R^{n+3}}{n+3} \left(1 - \frac{D}{R} \right)^{n+3} \iint_{\sigma} \delta\rho(Q) \left[\left(1 + \frac{kH(Q)}{R-D} \right)^{n+3} - 1 \right] \bar{R}_{nm}(Q) d\sigma(Q), \quad (2-6b)'$$

respectively.

The compensation "factor" k

This concept of isostasy is based on the principle of mass balance: surplus + deficit = 0. In the simple Airy/Heiskanen isostatic model this enables us to derive the geometry of the compensation surface (roots/antiroots) such that an exact 1 : 1 relation is postulated between a topographic height H and the corresponding compensation height kH . This mass balance principle, applied to rock topography and its compensation, yields

$$\rho_0 R^3 \left[\left(1 + \frac{H}{R} \right)^3 - 1 \right] + (\rho_0 - \rho_1) (R - D)^3 \left[1 - \left(1 + \frac{kH}{R - D} \right)^3 \right] = 0, \quad (2-7)$$

and after elementary manipulations

$$\frac{kH}{R - D} = \left\{ 1 - \left(1 - \frac{D}{R} \right)^{-3} k_0 \left[\left(1 + \frac{H}{R} \right)^3 - 1 \right] \right\}^{\frac{1}{3}} - 1 \quad \dots \text{rock}; \quad (2-7a)$$

for the ocean and its compensation we obtain a similar expression,

$$\frac{kH}{R - D} = \left\{ 1 - \left(1 - \frac{D}{R} \right)^{-3} k_0 \left(1 - \frac{\rho_w}{\rho_0} \right) \left[\left(1 + \frac{H}{R} \right)^3 - 1 \right] \right\}^{\frac{1}{3}} - 1 \quad \dots \text{ocean} \quad (2-7b)$$

$$\text{with } k_0 = \frac{\rho_0}{(\rho_1 - \rho_0)}.$$

It is instructive to investigate the planar case. For this purpose we evaluate kH in a power series with respect to H ,

$$k = -\left(1 - \frac{D}{R}\right)^{-2} k_0 \frac{H}{R} + O\left(\frac{H}{R}\right),$$

and if we let the radius R become infinite, we obtain

$$k = -k_0 c_H \tag{2-8}$$

with $c_H = 1$ for $H > 0$ and $c_H = 1 - \frac{\rho_w}{\rho_0}$ for $H < 0$.

It is obvious that the compensation factor k is constant in the planar model and independent of both H and D . For standard densities $\rho_0 = 2.67$, $\rho_1 = 3.27$, $\rho_w = 1.03 \text{ gcm}^{-3}$, we obtain the familiar values of -4.45 and -2.73 for rock and ocean compensation, respectively (HM p.136). In the spherical model the compensation "factor" k is no longer a constant; it is a function which depends to a small extent on both the height H and the depth of the compensation level D according to (2-7a,b) with (2-8) as the leading term. In order to simplify, we introduce "normalized" heights \bar{H} and \bar{H}' according to

$$\begin{aligned} \bar{H} &= \frac{H}{R} \\ \bar{H}' &= \frac{kH}{R - D} \end{aligned} \tag{2-9}$$

and the earth's mass M by

$$M \doteq \frac{4\pi R^3}{3} \rho_M \tag{2-10}$$

with the mean earth density $\rho_M = 5.517 \text{ gcm}^{-3}$. With this notation, the topographic-isostatic potential in its harmonic series representation is given by

$$T_{TI}(P) = \frac{GM}{\Gamma_P} \sum_{n=1}^{\infty} \left(\frac{R}{\Gamma_P}\right)^n \sum_{m=-n}^n \bar{T}_{nm} \bar{R}_{nm}(P) \tag{2-11}$$

with the harmonic (Fourier) coefficients of the topographic-isostatic potential

$$\bar{T}_{nm} := \bar{T}_{nm}^{(t)} + \bar{T}_{nm}^{(c)}, \quad (2-12a)$$

$$\bar{T}_{nm}^{(t)} := \frac{3\rho_0}{\rho_H} \frac{1}{(2n+1)(n+3)} \frac{1}{4\pi} \iint_{\sigma} c_H [[1 + \bar{H}(Q)]^{n+3} - 1] \bar{R}_{nm}(Q) d\sigma(Q), \quad (2-12b)$$

$$\bar{T}_{nm}^{(c)} := \frac{3\rho_0}{\rho_H} \frac{1}{(2n+1)(n+3)} \left(1 - \frac{D}{R}\right)^{n+3} k_0^{-1} \frac{1}{4\pi} \iint_{\sigma} [[1 + \bar{H}'(Q)]^{n+3} - 1] \bar{R}_{nm}(Q) d\sigma(Q) \quad (2-12c)$$

(Here "t" stands for topography and "c" for its compensation.) Note that the summation in (2-11) starts with $n = 1$ due to the mass equality condition; the reader is invited to check that $\bar{T}_{00}^{(t)} + \bar{T}_{00}^{(c)}$ is indeed equal to zero (hint: use (2-7a,b)).

3. APPROXIMATIONS FOR THE HARMONIC COEFFICIENTS OF THE TOPOGRAPHIC-ISOSTATIC POTENTIAL

3.1 Linear Approximation

Given a worldwide digital terrain model (DTM) representing the geometry of the solid earth surface, $H(Q)$, standard numerical integration techniques have been used in the past (Khan, 1973; Lachapelle, 1975). Due to the excessive computation requirements, only low degree coefficients (up to degree and order 36) using a $5^\circ \times 5^\circ$ DTM, could be determined. A couple of years ago, Colombo developed a fast Fourier algorithm for the sphere which can be efficiently applied if the integrand is independent of any degree n . Unfortunately, this is not the case with (2-12b,c). However, due to the smallness of \bar{H} and \bar{H}' compared to 1, a linear approximation seemed to be justified, yielding integrands

$$\frac{1}{n+3} [(1 + \bar{H})^{n+3} - 1] \doteq \bar{H}, \quad (3-1)$$

$$\frac{1}{n+3} [(1 + \bar{H}')^{n+3} - 1] \doteq \bar{H}',$$

which are obviously independent of the degree n . Therefore, in the linear approximation, the FFT algorithm applied to \bar{H} and \bar{H}' , respectively, can be and has been used (Rapp, 1982), providing the Fourier coefficients

$$\frac{1}{4\pi} \iint_{\sigma} c_H \bar{H}(Q) \bar{R}_{nm}(Q) d\sigma(Q), \quad (3-2)$$

$$\frac{1}{4\pi} \iint_{\sigma} \bar{H}'(Q) \bar{R}_{nm}(Q) d\sigma(Q),$$

in a very efficient way.

In this linear approximation case, the product $c_H H$ is usually called "equivalent rock topography" which, loosely speaking, trades in rock for water. The products $\rho_0 c_H H$ and $\rho_0 k_0^{-1} H'$ can consequently be interpreted as surface layer densities at zero level and at the level of compensation. Therefore, in the linear approximation, the topographic-isostatic potential is represented in

terms of a double layer potential.

The linear approximation of (2-12b) yields

$$\bar{T}_{nm}^{(t)} \doteq \frac{3\rho_0}{R\rho_H} \frac{1}{(2n+1)} \frac{1}{4\pi} \iint_{\sigma} c_H H(Q) \bar{R}_{nm}(Q) d\sigma(Q); \quad (3-3a)$$

the linear term of (2-7b) is

$$\bar{H}' \doteq -\left[1 - \frac{D}{R}\right]^{-3} k_0 c_H \bar{H}$$

leading to

$$\bar{T}_{nm}^{(c)} \doteq -\frac{3\rho_0}{R\rho_H} \frac{1}{(2n+1)} \left[1 - \frac{D}{R}\right]^n \frac{1}{4\pi} \iint_{\sigma} c_H H(Q) \bar{R}_{nm}(Q) d\sigma(Q). \quad (3-3b)$$

Adding $\bar{T}_{nm}^{(t)}$ and $\bar{T}_{nm}^{(c)}$ according to (2-12a) the harmonic series of the topographic-isostatic potential's linear approximation is given by

$$T_{TI}(P) \doteq \frac{4\pi GR\rho_0}{r_p} \sum_{n=1}^{\infty} \left(\frac{R}{r_p}\right)^n \frac{1}{2n+1} \left[1 - \left[1 - \frac{D}{R}\right]^n\right] \sum_{m=-n}^n \bar{R}_{nm}(P) \frac{1}{4\pi} \iint_{\sigma} c_H H(Q) \bar{R}_{nm}(Q) d\sigma(Q) \quad (3-4)$$

Exactly the same expression can be obtained if rock/ocean and compensation masses are considered as single layers at zero level and at the level of compensation, respectively.

Equation (3-4) is well suited to discuss the two extreme cases of $D = 0$ and $D = R$. It is obvious that for $D = 0$ the topographic-isostatic potential in its linear approximation vanishes identically. For the second case, $D = R$, the topographic-isostatic potential reduces to the topographic potential with vanishing zero degree harmonic (due to the mass balance). Neither of these two cases is realistic, as we know from geodetic and geophysical evidence. If we consider "reasonable" values of $0 < D \ll R$, we may (at least for low degrees) approximate

$$\left[1 - \frac{D}{R}\right]^n \doteq 1 - n \frac{D}{R}; \quad (3-5)$$

we observe that the main terms in (3-4) cancel each other and obtain the approximation

$$T_{TI}(P) \doteq \frac{4\pi GDR\rho_0}{r_p} \sum_{n=1}^{\infty} \left(\frac{R}{r_p}\right)^n \frac{n}{2n+1} \sum_{m=-n}^n \bar{R}_{nm}(P) \frac{1}{4\pi} \iint_{\sigma} c_H H(Q) \bar{R}_{nm}(Q) d\sigma(Q) \quad (3-6)$$

which can be further simplified with

$$\frac{n}{2n+1} \doteq \frac{1}{2} \quad (3-7)$$

and the harmonic representation of the equivalent rock topography,

$$c_H H(P) = \sum_n \sum_m \bar{R}_{nm}(P) \frac{1}{4\pi} \iint_{\sigma} c_H H(Q) \bar{R}_{nm}(Q) d\sigma(Q), \quad (3-8)$$

we find at zero level

$$\boxed{T_{TI}(P) \doteq 2\pi G D \rho_0 c_H H(P)} \quad (3-9)$$

(cf. also HM, p. 149). This approximative formula is a very useful rule of thumb which provides a fairly good estimate for a standard Airy/Heiskanen isostatic model. From this simple expression we conclude that the *topographic-isostatic potential is approximately linearly dependent on the depth of compensation and also linearly on the height of the equivalent rock topography.*

3.2 Higher order approximations

Rapp's (1982) argument that the efficient FFT algorithm is only applicable in the linear approximation, which we have shown is the double layer formulation, is no longer valid if we use the binomial expansion of the left-hand side of (3-1),

$$(1 + \bar{H})^{n+3} - 1 = \sum_{j=1}^{n+3} \binom{n+3}{j} \bar{H}^j \quad (3-10)$$

(analogous for \bar{H}'), yielding exact expressions (within spherical approximation) of the harmonic coefficients of the rock/ocean topography and its isostatic

compensation:

$$\bar{T}_{nm}^{(t)} = \frac{3\rho_0}{\rho_H} \frac{1}{(2n+1)(n+3)} \sum_{j=1}^{n+3} \binom{n+3}{j} \frac{1}{4\pi} \iint_{\sigma} c_H \bar{H}^j(Q) \bar{R}_{nm}(Q) d\sigma(Q) \quad (3-11a)$$

$$\bar{T}_{nm}^{(c)} = \frac{3\rho_0}{\rho_H} \frac{1}{(2n+1)(n+3)} \left(1 - \frac{D}{R}\right)^{n+3} k_{\sigma}^{-1} \sum_{j=1}^{n+3} \binom{n+3}{j} \frac{1}{4\pi} \iint_{\sigma} c_H \bar{H}'^j(Q) \bar{R}_{nm}(Q) d\sigma(Q) \quad (3-11b)$$

There is no reason why FFT could not be applied to any power of \bar{H} and \bar{H}' , respectively. (Note that (3-11a,b) are exact.) But do we gain anything by employing FFT, considering the fact that $2(n+3)$ FFT's have to be performed (one FFT for each power of \bar{H} and \bar{H}'), compared to twice a standard numerical integration? In the case of our earth we know that $\bar{H}, \bar{H}' \ll 1$; therefore, (3-10) converges very quickly and we can safely terminate the binomial expansion at a very low degree without committing a significant error (an upper limit of power $j = 5$ is perfectly sufficient). Consequently, only a small number of FFT's must be calculated; we typically save a tremendous amount of computer time without sacrificing accuracy, and can arbitrarily improve the result by adding another power of \bar{H} and \bar{H}' if we so desire.

3.3 The second order effect

By the second order effect we understand the contribution of the second power of \bar{H} and \bar{H}' to the topographic-isostatic potential. Because of the rapid convergence of (3-10), this second order effect represents with very good approximation the difference between the actual topographic-isostatic potential and its double layer approximation. Is this difference sufficiently small to be safely neglected?

Actually, there are two kinds of second order effects: one is due to the second power of \bar{H} and \bar{H}' in the binomial expansion (3-10), the other is due to the second power of \bar{H} in the compensation function $k = k(H)$ of (2-7a,b).

The second order effect due to rock/ocean topography is straightforward: using the binomial expansion (3-10) in (2-12b) and observing the binomial

coefficient

$$\frac{1}{(n+3)} \binom{n+3}{2} = \frac{(n+2)}{2},$$

we obtain

$$\delta \bar{T}_{nm}^{(t)} = \frac{3\rho_0}{2\rho_M} \frac{n+2}{(2n+1)} \frac{1}{4\pi} \iint_{\sigma} c_H \bar{H}^2(Q) \bar{R}_{nm}(Q) d\sigma(Q). \quad (3-12a)$$

For the compensation part we develop (2-7a,b) in a series up to the second power of H,

$$\left(1 - \frac{D}{R}\right)^3 \bar{H}' = -k_0 c_H \bar{H} (1 + \bar{H}) - k_3^2 c_H^2 \bar{H}^2 \left(1 - \frac{D}{R}\right)^{-3} + O(\bar{H}^3),$$

and using again the binomial expansion (3-10), we get

$$\frac{n+2}{2} \left(1 - \frac{D}{R}\right)^3 \bar{H}' = \left(\frac{n}{2} + 1\right) k_3^2 c_H^2 \bar{H}^2 \left(1 - \frac{D}{R}\right)^{-3} + O(\bar{H}^3)$$

and obtain as second order contribution of the isostatic compensation

$$\delta \bar{T}_{nm}^{(c)} = \frac{3\rho_0}{\rho_M} \frac{1}{(2n+1)} \left(1 - \frac{D}{R}\right)^n \frac{1}{4\pi} \iint_{\sigma} c_H \bar{H}^2 \left[\frac{n}{2} k_0 c_H \left(1 - \frac{D}{R}\right)^{-3} - 1 \right] \bar{R}_{nm}(Q) d\sigma(Q). \quad (3-12b)$$

Synthesizing $T_{nm}^{(t)}$ and $\delta \bar{T}_{nm}^{(c)}$ according to (2-11), we obtain the second order effect of the topographic-isostatic potential,

$$\delta T_{TI}(P) = \frac{GM}{r_P} \sum_{n=1}^{\infty} \left(\frac{R}{r_P}\right)^n \sum_{m=-n}^n \delta \bar{T}_{nm} \bar{R}_{nm}(P) \quad (3-13)$$

with the harmonic coefficients

$$\begin{aligned} \delta \bar{T}_{nm} &:= \delta T_{nm}^{(t)} + \delta T_{nm}^{(c)} \\ &= \frac{3\rho_0}{\rho_M} \frac{1}{(2n+1)} \frac{1}{4\pi} \iint_{\sigma} c_H \bar{H}^2 \left\{ \left(\frac{n}{2} + 1\right) + \left(1 - \frac{D}{R}\right)^n \left[\frac{n}{2} k_0 c_H \left(1 - \frac{D}{R}\right)^{-3} - 1 \right] \right\} \bar{R}_{nm} d\sigma. \end{aligned} \quad (3-14)$$

Using the approximations (3-5) and (3-7), this odd-looking expression can be

considerably simplified if we admit an error on the order of 20%, which can be accepted since the second order effect is small compared to the first order effect, yielding

$$\delta \bar{T}_{nm} \doteq \frac{3\rho_0}{4\rho_M} k_0 \frac{1}{4\pi} \iint_{\sigma} [c_H \bar{H}(Q)]^2 \bar{R}_{nm}(Q) d\sigma(Q). \quad (3-14)'$$

With (3-13) we then obtain at zero level

$$\delta T_{II}(P) \doteq \frac{GM}{4R^3} \frac{3\rho_0}{\rho_M} k_0 \sum_{n=1}^{\infty} \sum_{m=-n}^n \bar{R}_{nm}(P) \frac{1}{4\pi} \iint_{\sigma} [c_H \bar{H}(Q)]^2 \bar{R}_{nm}(Q) d\sigma(Q)$$

and replacing M by (2-10), the approximated second order effect on the topographic-isostatic potential is simply

$$\delta T_{II}(P) \doteq \pi G \rho_0 k_0 [c_H \bar{H}(P)]^2 \quad (3-15)$$

We observe that under these approximations the second order effect is independent of the depth of compensation, is proportional to the square of the equivalent rock topography's height, and is therefore always positive.

If we use the standard values for ρ_0 , ρ_1 , and ρ_M , we obtain a rule of thumb formula for the second order effect on the topographic-isostatic geoidal height, using the Bruns formula,

$$\delta N_{II}[m] \doteq 0.2 H_{[km]}^{*2} \quad (3-16)$$

with $H^* = c_H \bar{H}$, the equivalent rock topography. Note the formal similarity to the Molodensky effect (HM, p. 328)!

Combining first and second order effects we obtain

$$T_{II}(P) \doteq 2\pi G D \rho_0 H^* \left(1 + k_0 \frac{H^*}{2D} \right) \quad (3-17)$$

from (3-17) we conclude that the second order effect, relative to the total

potential, increases with decreasing depth of compensation and vice versa. For areas with extreme topography (both positive and negative), the second order effect may amount to about 50% of the first order effect and certainly cannot be neglected.

4. POWER SPECTRUM CONSIDERATIONS

The power spectrum (degree variances) of the topographic-isostatic potential in linear approximation is implied by the harmonic coefficients $\bar{T}_{nm}^{(t)}$ and $\bar{T}_{nm}^{(c)}$ of (3-3a,b),

$$\bar{T}_n^2 := \sum_{m=-n}^n (\bar{T}_{nm}^{(t)} + \bar{T}_{nm}^{(c)})^2. \quad (4-1)$$

Denoting the harmonic coefficients of the normalized equivalent rock topography by \bar{H}_{nm}^* ,

$$\bar{H}_{nm}^* := \frac{1}{4\pi} \iint_{\sigma} c_H \frac{H(Q)}{R} \bar{R}_{nm}(Q) d\sigma(Q), \quad (4-2)$$

the degree variances of the topographic-isostatic potential \bar{T}_n^2 are related to the degree variances of the equivalent rock topography \bar{H}_n^{*2} ,

$$\bar{H}_n^{*2} := \sum_{m=-n}^n \bar{H}_{nm}^{*2} \quad (4-3)$$

by

$$\bar{T}_n^2 = \left\{ \frac{3\rho_g}{\rho_H} \frac{1}{2n+1} \left[1 - \left(1 - \frac{D}{R} \right)^n \right] \right\}^2 \bar{H}_n^{*2} \quad (4-4)$$

(cf. Lambeck, 1979, p. 592).

Considering \bar{T}_n^2 as a function of the compensation depth D , it is obvious that the power spectrum of the topographic-isostatic potential is gaining power with increasing compensation depth and attains a maximum for $D = R$ such that in this extreme case \bar{T}_n^2 reduces to the degree variance of the potential of the topography for $n > 0$ ($\bar{T}_n^2 = 0$ in any case). For moderately large depths and low degrees n we may use the approximation (3-5) and obtain as ratio between

topographic-isostatic degree variances, corresponding to the compensation depths D_1 and D_2 ,

$$\frac{\bar{T}_n^2(D_1)}{\bar{T}_n^2(D_2)} \doteq \frac{D_1}{D_2} \quad (4-5)$$

From geodetic satellite and surface data we know that the actual anomalous gravitational potential of the earth has much less power than $\{\bar{T}_n^2(D = R)\}$, implying that the rock/ocean topography is isostatically compensated to a large extent with a relatively small D . A global standard value of 30 km is generally accepted and frequently used for the purpose of topographic-isostatic reduction of surface data.

If the global figure for the compensation depth is D , we should expect a good agreement between the power spectrum of the earth's anomalous gravitational potential \bar{V}_n^2 and the power spectrum $\bar{T}_n^2(D)$, provided that the standard Airy/Heiskanen model describes reality sufficiently well.

This idea was pursued by Rapp (1982a), using the simple double layer model (linear approximation) and the DTM data set consisting of 64800 $1^\circ \times 1^\circ$ mean elevation and ocean depth data, provided by DMAAC. His results clearly demonstrate that the standard Airy/Heiskanen compensation model with a compensation depth of $D = 30$ km produces much too little power over the entire frequency range from $n = 2$ to 180 and is totally inadequate to explain the observed power spectrum of the anomalous gravitational potential. Later investigations by Rapp and Rummel (private communication), using in addition the terms of second and third order in \bar{H} , confirmed the earlier studies.

Guided by the relation (4-4) or (4-5), considerably larger values for D were suggested by Rapp (1982a). Obviously the best agreement between the two power spectra was achieved for a compensation depth of $D = 50$ km, yielding a good match between degree 50 and 150; poor results have been obtained for the range between 20 and 50 km, but what is particularly astonishing, also in the high frequency part between degree 150 and 180. Moreover, a compensation depth of 50 km is generally considered to be too large by a factor of almost 2 and is geophysically hard to justify.

The South Pacific area has not only a strong appeal to financially sound vacationers but also to hard working geodesists (don't be misled by this coincidence!) because of extreme gravity field structures. Forsberg (1984) studied the topographic-isostatic geoid in the Tonga Trench and Tahiti area using the recently released 5' x 5' "SYNBAPS" ocean depth data set. (I strongly recommend to study Forsberg's report - it is a beautiful document!) His results, which are also based on the standard Airy/Heiskanen compensation model, also suggest much deeper compensation levels than 30 km. Forsberg argues that at smaller depths of 30 km or so, conventional isostasy is led ad absurdum by deep ocean trenches which would imply antiroots ending considerably above the actual ocean bottom(!) - an argument in favor of larger compensation depths. On the other hand, the observed average thickness of the crust below the ocean bottom is only about 6-8 km - a fact which would favor a compensation depth smaller than 30 km.

Isn't there a simple way out of that isostatic dilemma?

4.1 Compensation Depth versus Smoothing

The recent studies of Rapp (1982a) and Forsberg (1984), but also an earlier work by Moritz (1968) and Schwarz (1976) have triggered my interest in this problem; but in particular it was the simple idea of Vening Meinesz (1939) that the actual compensation takes place regionally rather than strictly locally, which made me to numerically investigate the problem of isostasy. But before we shall hit the target in Chapter 5, let's make a small sidestep to collocation.

During the collocation "high noon" period in the mid-seventies, one of the main issues was how to deal with block mean gravity anomalies within a homogeneous and isotropic statistical model environment. Numerical integration of the covariance function was prohibitive; therefore, an approximation had to be employed: through formally replacing the block averaging operator by a homogeneous and isotropic moving average operator of constant weight, the comfort of homogeneity and isotropy can be achieved. According to the convolution theorem, the moving average convolution process in the space

domain corresponds to a simple product between the eigenvalues of the moving average operator and the Fourier coefficients of the function to be averaged in the frequency domain. As far as collocation is concerned, this particular function is the kernel function (in least-squares collocation the covariance function) which, smoothed and unsmoothed, has to be represented by a finite and as simple as possible expression in order to render possible a fast calculation of linear functionals. Unfortunately, the eigenvalues of the moving average operator prevent such a closed expression and therefore, they have to be approximated by another spectrum which behaves properly. Schwarz (1976, p. 37 ff.) suggested replacing the moving average eigenvalues with the eigenvalues of an upward continuation operator. Applying this trick means that the statistical properties of mean values at zero level are replaced by the statistical properties of point values at a certain altitude which depends on the block size of the moving average operator. Numerical tests confirmed that this approximation was admissible.

Have we lost our track? No, we haven't! The same idea can be carried over to get, at least partially, out of the isostatic dilemma: assuming that the Vening Meinesz concept of regional isostatic compensation is correct, we may expect a reasonably good solution in terms of a power spectrum agreement (between the observed anomalous gravitational and the isostasy implied potential) by formally replacing the *regional isostatic concept of Vening Meinesz at compensation depth D_1* , by the *strictly local isostatic concept of Airy/Heiskanen at a larger depth D_2* , where $(D_2 - D_1)$ depends on the characteristics of the Vening Meinesz smoothing.

After that verbal avalanche, it is time to be a little more specific: confining ourselves to the linear approximation, the Airy/Heiskanen power spectrum is given by (4-4) which we repeat here

$$\bar{T}_n^2 = \left\{ \frac{3\rho_a}{\rho_M} \frac{1}{2r+1} \left[1 - \left(1 - \frac{D}{R} \right)^n \right] \right\}^2 \bar{H}_n^{*2} .$$

The regional Vening Meinesz concept is based on a smoothing of the compensation (= root/antiroot) surface. Since we don't know any better, we propose democratic smoothing represented by a homogeneous and isotropic

operator B with eigenvalues β_n ,

$$B(P, Q) = \frac{1}{4\pi} \sum_{n=0}^{\infty} (2n + 1) \beta_n P_n(\cos \psi_{PQ}), \quad (4-6a)$$

$$\beta_n = 2\pi \int_{-1}^1 B(t) P_n(t) dt \quad (t := \cos \psi), \quad (4-6b)$$

with $\beta_0 = 1$ to make the integral of the operator B over the unit sphere equal to 1 which is required for mass balance.

The operator B will now be applied to the equivalent rock topography represented by its harmonic coefficients \bar{H}_{nm}^* , at the compensation level only. Note: the rock/ocean topography remains unchanged, only the compensating masses and therefore, the compensation root/antiroot surface is smoothed. This smoothing process (which is a simple convolution in the space domain) is represented by a multiplication of \bar{H}_{nm}^* by the eigenvalue β_n ,

$$B * \bar{H}^* \longleftrightarrow \beta_n \cdot \bar{H}_{nm}^* \quad (4-7)$$

Therefore, the Vening Meiness power spectrum in its linear approximation is given by

$$\bar{T}_n^2(D_1) = \left\{ \frac{3\rho_o}{\rho_M} \frac{1}{2n+1} \left[1 - \left(1 - \frac{D_1}{R} \right)^n \beta_n \right] \right\}^2 \bar{H}_n^{*2}. \quad (4-8)$$

At this point we should briefly discuss two extreme cases of smoothing:

a) $\beta_n = 1 \quad \forall n = 0, 1, \dots$

In this case the smoothing operator B of equation (4-6a) degenerates into the Dirac distribution and will reproduce the input; consequently there is no smoothing involved. Therefore, this operator represents the standard Airy/Heiskanen model.

b) $\beta_0 = 1, \beta_n = 0 \quad \forall n = 1, 2, \dots$

In this case the smoothing operator B degenerates into the global average

operator with equal weight; the compensation masses form a homogeneous layer which is equivalent to a point mass at the origin. Therefore, this operator represents the extreme case of the Airy/Heiskanen model with $D_2 = R$.

It is evident that the two power spectra \bar{T}_n^2 and \bar{T}_n^2 coincide if the condition

$$\left(1 - \frac{D_1}{R}\right)^n \beta_n = \left(1 - \frac{D_2}{R}\right)^n \quad (4-9)$$

is fulfilled for all n . This implies an Airy/Heiskanen compensation depth D_2 .

$$D_2 = R - (R - D_1) \beta_n^{\frac{1}{n}}, \quad (4-10)$$

or, in terms of radius of compensation, $R_1 := R - D_1$,

$$R_2 = R_1 \beta_n^{\frac{1}{n}}. \quad (4-10)'$$

It is obvious that R_2 is constant (independent of the degree n) if and only if

$$\beta_n^{\frac{1}{n}} = b = \text{const.},$$

which implies

$$\beta_n = b^n \quad (4-11)$$

with $b < 1$ because of the compressing properties of a smoothing operator. The smoothing operator B corresponding to (4-11) is obtained by an inverse Fourier transform according to (4-6a)

$$B(P, Q) = \frac{1}{4\pi} \sum_{n=0}^{\infty} (2n + 1) b^n P_n(\cos \psi_{PQ}) \quad (4-12a)$$

which is evidently the interior Poisson operator (HM, p. 35). With $b = R_2/R_1$ (equation (4-10)' and (4-11)) we finally obtain

$$B(P, Q) = \frac{R_1 (R_1^2 - R_2^2)}{4\pi \Delta^3(P, Q)} \quad (4-13)$$

with the spatial distance s defined by

$$s(P,Q) = (R_1^2 + R_2^2 - 2R_1R_2\cos\psi_{PQ})^{1/2}.$$

We conclude: if the Vening Meinesz regional smoothing of the compensation surface is of Poisson type at level R_1 with parameter R_2 , we can exactly replace it by the standard Airy/Heiskanen model with compensation level R_2 . Or vice versa, using a standard Airy/Heiskanen model at depth D_2 corresponds exactly to the use of a Vening Meinesz model at depth D_1 with the Poisson smoothing (4-13) and parameter D_2 .

Now we are already on much safer ground because we are able to justify the formal use of an unusually large compensation depth. However, the crucial question is still open: does the Poisson smoothing reflect physical reality?

5. AN OPTIMAL VENING MEINESZ ISOSTATIC MODEL

If we are talking about "optimal", we have to choose a norm which defines what "good" is. The choice of the norm is not so difficult if we are primarily interested in the power spectrum of the topographic-isostatic potential. In this case we consider a solution good if its deviation from the observed power spectrum of the anomalous gravitational potential is small. Therefore, it is quite natural to look after an operator, acting on the compensation, which makes both spectra match as closely as possible.

From our considerations in Chapter 4, we conclude that the minimum number of parameters must be 2 if we are after a compensation smoothing operator: one parameter that controls the level of compensation, the second one controlling the smoothing. (Note that also the Poisson smoothing operator (4-13) has two parameters, R_1 and R_2 .)

5.1 Estimation of the parameters of the smoothing operator

In linear approximation, the Vening Meinesz topographic-isostatic power spectrum is given by equation (4-8); the operator's two parameters are D and b , where D stands for depth of compensation and b is a smoothing parameter (note that β_n depends on b). As a matter of fact, the individual harmonic coefficients of the topographic-isostatic potential are also controlled in the same way,

$$\bar{T}_{nm} = \bar{T}_{nm}(D, b). \quad (5-1)$$

Extending a suggestion of Tscherning (1984), we perform a least-squares estimation of the model parameters such that the energy of the residual field is minimized.

$$\left| \bar{T} - \bar{V} \right|^2 = \min. \quad (5-2)$$

Since the low order harmonics of the anomalous gravitational potential are to a large degree due to density disturbances in the upper mantle, and probably

due to even deeper sources, it makes no sense (and would only disturb the isostatic concept) to include the very long wavelength part in the energy budget.

With a homogeneous and isotropic smoothing operator B having eigenvalues β_n , the harmonic coefficients of the topographic-isostatic potential are given by

$$\bar{T}_{nm}^2(D, b) = \frac{3\rho_a}{\rho_M} \frac{1}{2n+1} \left[1 - \left(1 - \frac{D}{R} \right)^n \beta_n(b) \right] \bar{H}_{nm}^* . \quad (5-3)$$

The decision of the model spectrum $\{\beta_n(b)\}$ can be based on correlation considerations between $\bar{T}_n^2(D, b)$ and \bar{V}_n^2 , requiring that

$$\bar{T}_n^2 = \bar{V}_n^2 , \quad (5-4)$$

and yielding empirical estimates

$$\beta_n' = \left(1 - \frac{D}{R} \right)^{-n} \left[1 - \frac{\rho_M}{3\rho_a} (2n+1) \frac{\bar{V}_n}{\bar{H}_n^*} \right] \quad (5-5)$$

which depend on the choice of D. The figures 6.3a-d on page 31 show graphs of this empirical frequency transfer function β_n' for several compensation depths D. As data the Rapp 81 geopotential model and the worldwide $1^\circ \times 1^\circ$ DTM model, supplied by DMAAC, have been used. All empirical frequency transfer functions β_n' , at least for geophysically reasonable compensation depths, strongly suggest a Gaussian model of type

$$\beta_n(b) = e^{-b^2 n^2} . \quad (5-6)$$

The solid curves represent the best fit of such a Gaussian model to the empirical frequency transfer function.

Having chosen a model for $\beta_n(b)$, it is a simple matter of least-squares adjustment with 2 parameters to solve for the "best" D and b. If we use non-equal weights p_n which depend on the degree like

$$p_n = \left(\frac{R}{GM} \right)^{-2} \frac{2n+1}{k_n} \quad (5-7)$$

with the model degree variances k_n and error variances of the harmonic coefficients of the anomalous potential modelled by

$$\sigma_n^2 = \left(\frac{K}{n-1} \right)^2, \quad K \dots \text{constant}, \quad (5-8)$$

according to Jekeli (1979, pp. 13, 14), we can even interpret the least-squares solution as a kind of least-squares collocation solution for the model parameters D and b (cf. Moritz, 1980, pp. 160, 161). (Here the data consists of the vector $l := \{\bar{V}_{nm}\}$.)

Because of (5-7) and (5-8) the signal and error covariance matrices C_s and C_n are diagonal, which implies that the energy

$$\sum_{n=n_0}^N \left[\left(\frac{R}{GM} \right)^2 \frac{k_n}{2n+1} + \left(\frac{K}{n-1} \right)^2 \right]^{-1} \sum_{m=-n}^n \left[\bar{T}_{nm}(D,b) - \bar{V}_{nm} \right]^2 \quad (5-9)$$

must be minimized with respect to D and b . With the Taylor linearization of \bar{T}_{nm}

$$\begin{aligned} \bar{T}_{nm}(D,b) &= \bar{T}_{nm}(D^{(0)}, b^{(0)}) + \frac{\partial \bar{T}_{nm}(D,b)}{\partial D} \bigg|_{(D=D^{(0)}, b=b^{(0)})} (D - D^{(0)}) \\ &\quad + \frac{\partial \bar{T}_{nm}(D,b)}{\partial b} \bigg|_{(D=D^{(0)}, b=b^{(0)})} (b - b^{(0)}) \end{aligned} \quad (5-10)$$

at an appropriate Taylor point (for example $D = 30$ km and b according to the solid line in Fig. 6.3b), we obtain the coefficients of the design matrix A . The elements of the two column vectors a_1 and a_2 consist of the partials of (5-10)

$$\begin{aligned} a_1 &= \left\{ \frac{\partial \bar{T}_{nm}(D,b)}{\partial D} \bigg|_{(D=D^{(0)}, b=b^{(0)})} \right\}, \\ a_2 &= \left\{ \frac{\partial \bar{T}_{nm}(D,b)}{\partial b} \bigg|_{(D=D^{(0)}, b=b^{(0)})} \right\}, \end{aligned} \quad (5-11)$$

the residual parameter vector X of

$$X^T := [\delta D, \delta b]. \quad (5-12)$$

The least-squares solution is provided by

$$\hat{X} = (A^T \bar{C}^{-1} A)^{-1} A^T \bar{C}^{-1} (l - l^{(o)}) \quad (5-13)$$

with

$$\bar{C} := C_m + C_n \quad (5-14)$$

and

$$l^{(o)} := \left\{ \overset{n}{T}_{nm}(D^{(o)}, b^{(o)}) \right\} \quad (5-15)$$

Finally we obtain the wanted parameters D and b of our best-fitting Vening Meinesz isostatic model,

$$\hat{D} = D^{(o)} + \delta D,$$

$$\hat{b} = b^{(o)} + \delta b.$$

For error considerations we have

$$E_{xx} = (A^T \bar{C}^{-1} A)^{-1} \quad (5-16)$$

as parameter error covariance matrix (for reference see Moritz (1980, Part B)).

5.2 Fine-tuning of parameter estimation

When we derived the least-squares estimation of the isostatic parameters D and b , we made two simplifications: firstly, if our Taylor point is far away from reality, we must iterate the estimation process; secondly, in our discussion of the estimation problem and in all our derivations we have generously and tacitly assumed that $\overset{n}{T}_{nm}$ of equation (5-3) is correct.

The first problem will not be dealt with here because it is simple and standard, provided the Taylor point is not too much off the truth. The second problem is probably slightly more delicate, although a relatively simple solution is possible:

Equation (5-3) presupposes a linear relation between the topographic- isostatic potential and the equivalent rock topography. But according to (2-11) and (2-12a,b,c) we know that the relation is highly non-linear. Therefore, the concept of parameter estimation has to be modified accordingly.

This modification is basically due to second and higher order effects which, we know from our discussion in Chapter 3, are small because the topographic height is so much smaller than the radius of the earth. Therefore, an iteration process offers itself again.

Let B be, as before, the smoothing operator applied to the compensation surface, represented by \bar{H}' , yielding the smoothed compensation surface $\bar{H}' = B * \bar{H}'$. Then \bar{H}' should be used for the harmonic coefficients of the compensation $\bar{T}_{nm}^{(c)}$ of equation (3-11b). Note, however, that \bar{H} (and not \bar{H}') is used for the harmonic coefficients of the topography $\bar{T}_{nm}^{(t)}$, because smoothing is only applied to the compensating masses. The problem is that also higher order powers of \bar{H}' enter into $\bar{T}_{nm}^{(c)}$,

$$\bar{T}_{nm}^{(c)} = \frac{3\rho_0}{\rho_H} \frac{1}{(2n+1)(n+3)} \left[1 - \frac{D}{R}\right]^{n+s} k_0^{-1} \sum_{j=1}^{n+3} \binom{n+3}{j} \frac{1}{4\pi} \iint_{\sigma} c_H \bar{H}'^j(Q) \bar{R}_{nm}(Q) d\sigma(Q) \quad (5-17)$$

while $\bar{T}_{nm}^{(t)}$ remains unchanged (equation (3-11a)). Since \bar{H}' is a convolution of B and \bar{H} , higher order powers of \bar{H} correspond to convolutions in the frequency domain. Therefore, the smoothing parameter b enters in a rather complicated manner into the higher order terms of $\bar{T}_{nm}^{(c)}$. But fortunately, these terms are only small correction terms to the leading linear term (5-3); therefore, if we solve for b , it will be sufficient to calculate the higher order terms based on the latest knowledge of b and to consider them formally as constants in the subsequent least-squares estimation process. It is sufficient to iterate this process a few times because of the extraordinarily rapid convergence. The entire procedure can be summarized as follows:

0) $i = 0$

harmonic analysis of low order powers of topography according to (3-11a); correlation study (5-5) yields initial estimates $\hat{D}^{(0)}$ and $\hat{b}^{(0)}$;

1) $i = i + 1$

smoothing of compensation surface ($\bar{H}'^{(i)} = B^{(i-1)} * \bar{H}'$) using $\hat{D}^{(i-1)}$ and $\hat{b}^{(i-1)}$;

2) Harmonic analysis of low order powers of smoothed compensation surface $\bar{H}'^{(i)}$ according to (5-17) yields a first order term $\bar{T}_{nm}^{(i)}$ which will be considered as a function of D and b , and higher order (correction) terms $\delta\bar{T}_{nm}^{(i)}$ which will be considered as constants in the subsequent step;

3) Adjustment (collocation) solution for D and b with Taylor point ($D^{(i-1)}$, $b^{(i-1)}$) and linearization restricted to the linear term $\bar{T}_{nm}^{(i)}$ of step (2); Stop if $|\hat{D}^{(i)} - \hat{D}^{(i-1)}| < \epsilon_D$ and $|\hat{b}^{(i)} - \hat{b}^{(i-1)}| < \epsilon_b$, else go to (1).

The result of this iteration process is both a best estimate for the depth of compensation and for the parameter of the most likely compensation smoothing, and a set of harmonic coefficients of the topographic-isostatic potential corresponding to that Vening Meinesz regional isostatic compensation model.

6. NUMERICAL STUDIES, RESULTS, CONCLUSIONS

For the numerical investigations the worldwide digital terrain model of 64800 $1^\circ \times 1^\circ$ mean elevations and ocean bottom depths (but no information on ice coverage), supplied by DMAAC in 1979, and, representing the earth's gravity field, the Rapp 1981 solution which is complete to degree and order 180, have been used. Due to the time limitations of this study it was unfortunately not possible to merge the recently released SYNAPS dataset, which consists of $5'$ by $5'$ mean ocean depths, with the available DTM. Since the output of a system can hardly be better than its input, our results have to be considered with these reservations in mind.

As we mentioned already at the beginning, the goal of this study was both the parameter estimation of the most likely isostatic compensation model and the determination of a set of topographic-isostatic coefficients complete up to degree and order 180, based on that compensation model. This task would be formidable without support of the powerful tool of fast Fourier transform on the sphere. Therefore, the unlimited access to Colombo's (1981) outstanding FFT algorithms "HARMIN" for analysis and "SSYNTH" for synthesis was particularly appreciated. The following is a comprehensive documentation of our numerical studies.

In all our investigations, the following parameters have been used:

density:

$$\rho_0 = 2.67 \text{ gcm}^{-3} \quad \dots \text{ rock topography}$$

$$\rho_w = 1.027 \text{ gcm}^{-3} \quad \dots \text{ ocean water}$$

$$\rho_1 = 3.27 \text{ gcm}^{-3} \quad \dots \text{ crust}$$

$$\rho_M = 5.517 \text{ gcm}^{-3} \quad \dots \text{ mean earth}$$

earth radius:

$$R = 6371 \text{ km}$$

potential coefficient degree variance model:

$$k_n = \left(\frac{A \cdot 10^{-6}}{n^B} \right)^2, \quad A = 4.1, \quad B = 1.8$$

(cf. Rapp, 1979, p. 10)

potential coefficient error model:

$$\sigma_n^2 = \left(\frac{K}{n-1} \right)^2, \quad K = 0.0581 \cdot 10^{-6}$$

(cf. Jekeli, 1979, p. 13 ff.)

harmonic series complete up to degree:

$$n = 180$$

binomial expansion up to power:

$$j = 5$$

In order to get an idea about the contribution of first and higher order terms to the harmonic coefficients of the topographic-isostatic potential, we provide in Fig. 6.1 a graph of the degree variances, separate for the linear and second order term as well as the composite degree variances. Note that the linear approximation pretends more power over the entire frequency range than the exact topographic-isostatic model actually has. The contribution of the third order term is already so small that it does not show up in the plotting window. Therefore, we have confined our discussion of higher order terms in Chapter 3 to the second order term only.

The dependence of the power spectrum on the choice of the compensation depth D or, if Poisson compensation smoothing is employed, on the corresponding smoothing parameter (cf. Section 4.1), is illustrated in Fig. 6.2 for depths $D = 30, 50, 70,$ and 100 km. The gain of power with increasing compensation depth (or more compensation smoothing) is obvious.

Frequency transfer functions between the Rapp 81 anomalous gravitational power spectrum and the topographic-isostatic power spectrum in linear

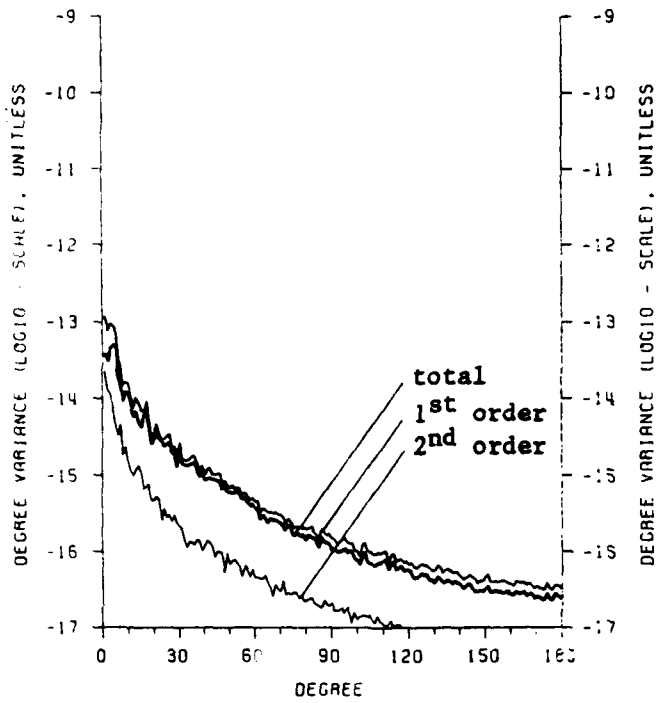


Fig. 6.1
 Degree variances of the
 topographic-isostatic
 potential, low-order terms
 and total (no compensation
 smoothing)

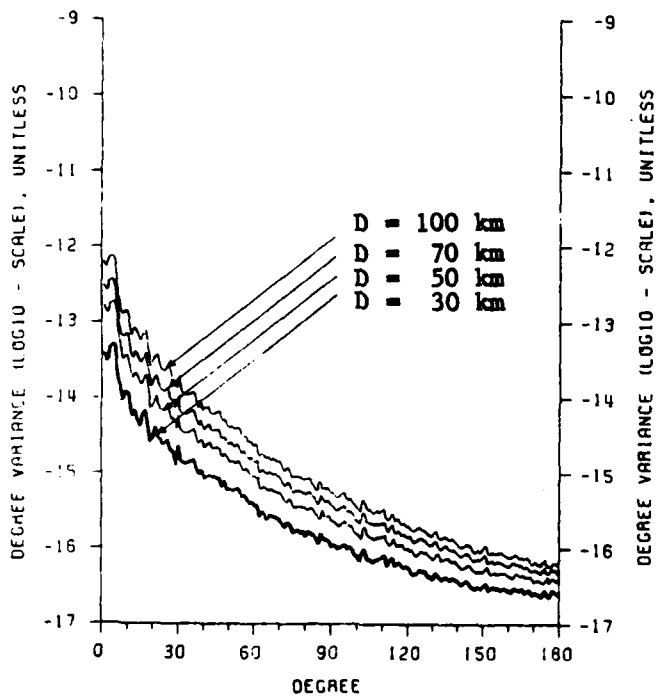


Fig. 6.2
 Degree variances of the
 topographic-isostatic
 potential as dependent on
 the depth D of compensation
 (no compensation smoothing)

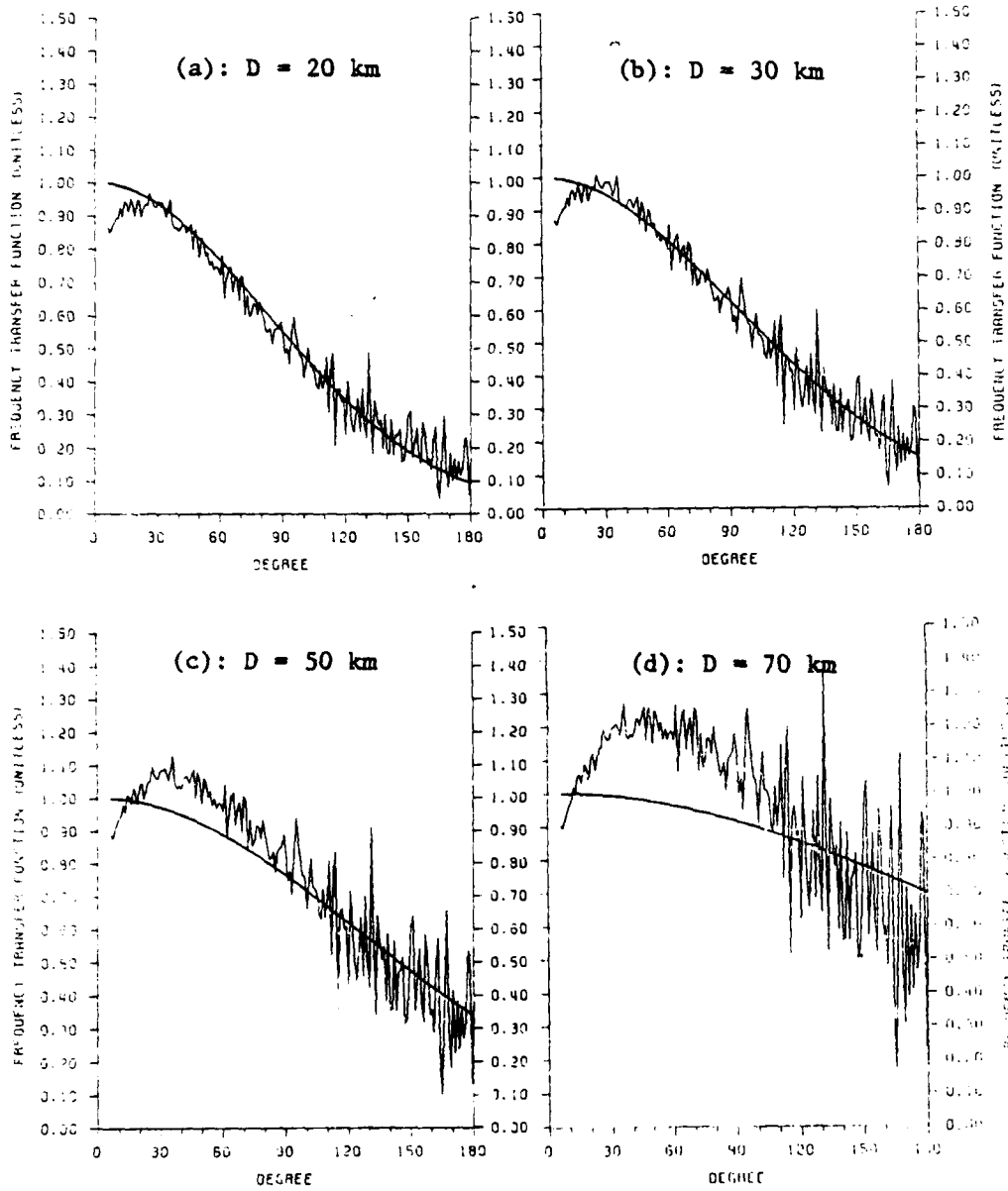


Fig. 6.3a-d Frequency transfer functions geopotential/topographic-isostatic potential as implied by various compensation depths D .

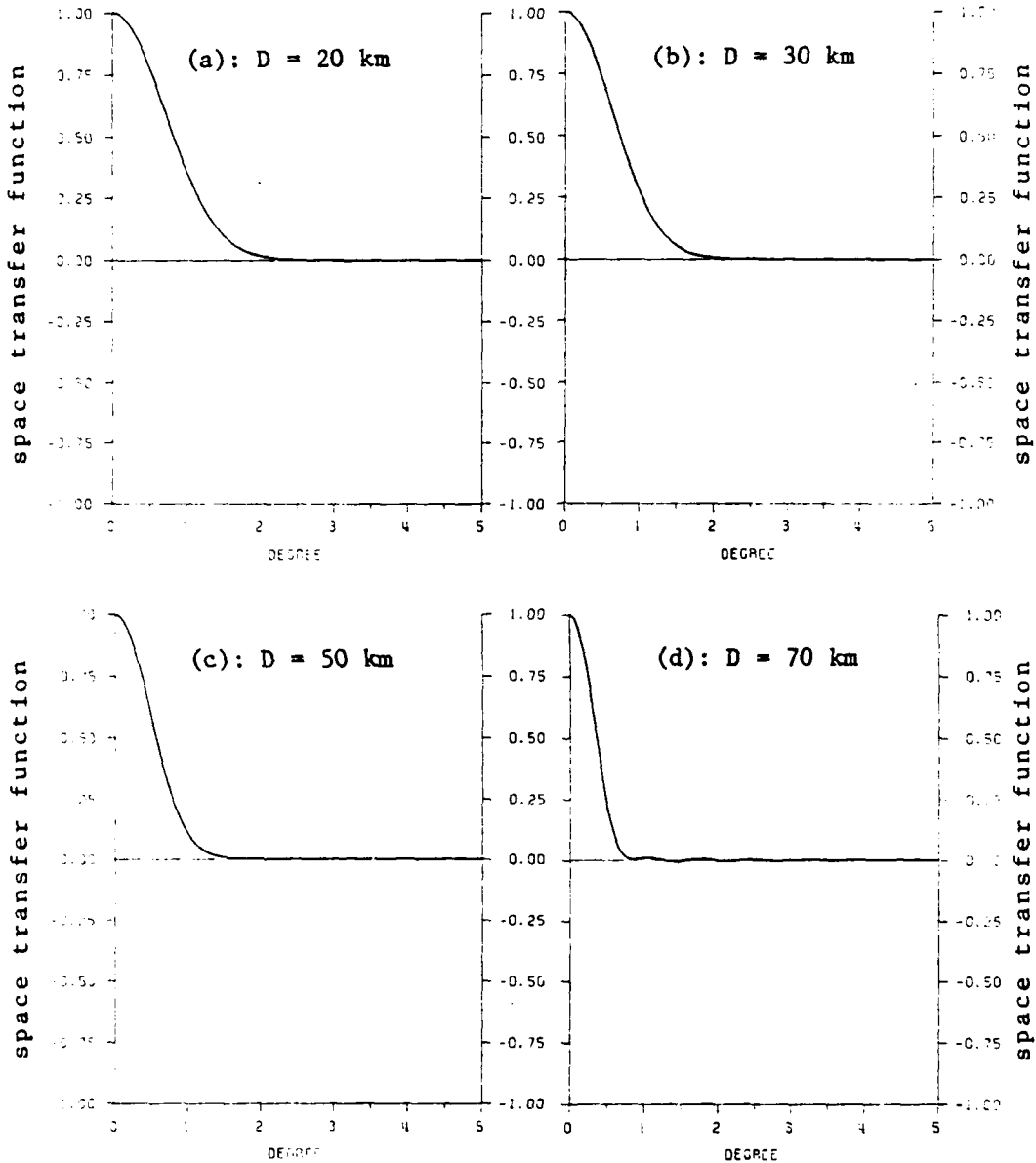


Fig. 6.4a-d Space transfer functions (= smoothing operators), as implied by various compensation depths D , depending on spherical distance.

approximation are given in Fig. 6.3a-d for compensation depths $D = 20, 30, 50,$ and 70 km. The graphs strongly suggest a Gaussian model of the type (5-6). The solid lines represent that best model fit.

By an inverse Fourier transform of the frequency transfer function β_n we obtain the corresponding space transfer function which is essentially the compensation smoothing operator B ,

$$B(P,Q) = \frac{1}{4\pi} \sum_{n=0}^{\infty} (2n + 1) \beta_n P_n(P,Q). \quad (6-1)$$

Using the best fitting Gaussian frequency transfer model, the smoothing operator has been determined for the most important part of its support and is presented in Fig. 6.4a-d normalized to $B(0) = 1$. The scale of the abscissa is arc deg. of spherical distance. These operators demonstrate that the smoothing of the compensation surface, as implied by our knowledge of the global gravitational field of the earth, is obviously most likely of Gaussian type rather than of moving average, box-shaped type or of Poisson type. The radius of smoothing (theoretically 180 degrees, practically very much smaller) decreases with increasing compensation depth. This should be expected because an increase of compensation depth accounts already for a certain degree of smoothing, although of Poisson type. For geophysically relevant compensation depths the smoothing radius does practically not exceed 2 degrees.

For the least-squares estimation of the two model parameters, compensation depth D and smoothing parameter b , the initial (Taylor) values

$$\begin{aligned} D^{(0)} &= 30 \text{ km}, \\ b^{(0)} &= 0.0082, \end{aligned} \quad (6-1)$$

suggested by the correlation pattern, have been used. (The smoothing parameter $b^{(0)} = 0.0082$ implies a "correlation length" of the bell-shaped Gaussian frequency transfer function of about (degree) $n = 100$.) Graphs of both the frequency and the corresponding space domain transfer function (smoothing operator) for these initial values are presented in Figs. 6.3b and 6.4b.

SPACE TRANSFER FUNCTION (= SMOOTHING OPERATOR)
BASED ON A 1 X 1 DEG. DTM (DMA-MODEL, 1979)
AND AIRY/VENING MEINESZ COMPENSATION MODEL WITH
GAUSSIAN SMOOTHING, PARAMETER B = 0.0091
DEPTH = 24 KM, ROCK DENSITY = 2.67 G/CM**3,
CRUST DENSITY = 3.27 G/CM**3,
WATER DENSITY = 1.027 G/CM**3

CALCULATION METHOD: FFT + POWER SERIES

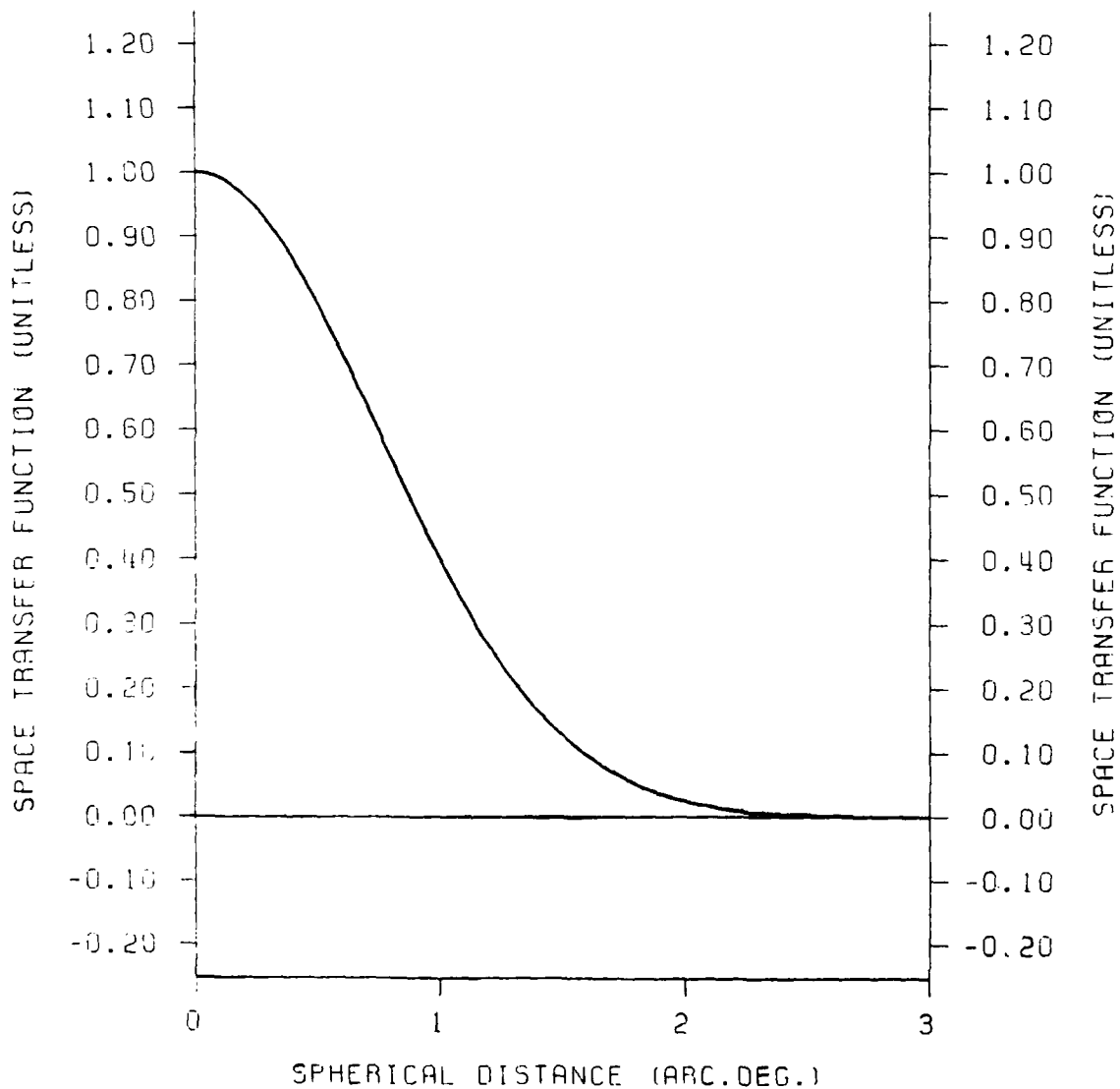


Fig. 6.5 Optimal smoothing operator

DEGREE VARIANCES OF THE TOPOGRAPHIC-ISOSTATIC POTENTIAL
 BASED ON A 1 X 1 DEG. DTM (DMA-MODEL, 1979)
 AND AIRY/VENING-MEINESZ COMPENSATION MODEL WITH
 ROOT/ANTIROOT SMOOTHING OF GAUSS TYPE, $b = 0.0091$,
 DEPTH = 24 KM, ROCK DENSITY = 2.67 G/CM³,
 CRUST DENSITY = 3.27 G/CM³,
 WATER DENSITY = 1.027 G/CM³

CALCULATION METHOD: FFT + POWER SERIES

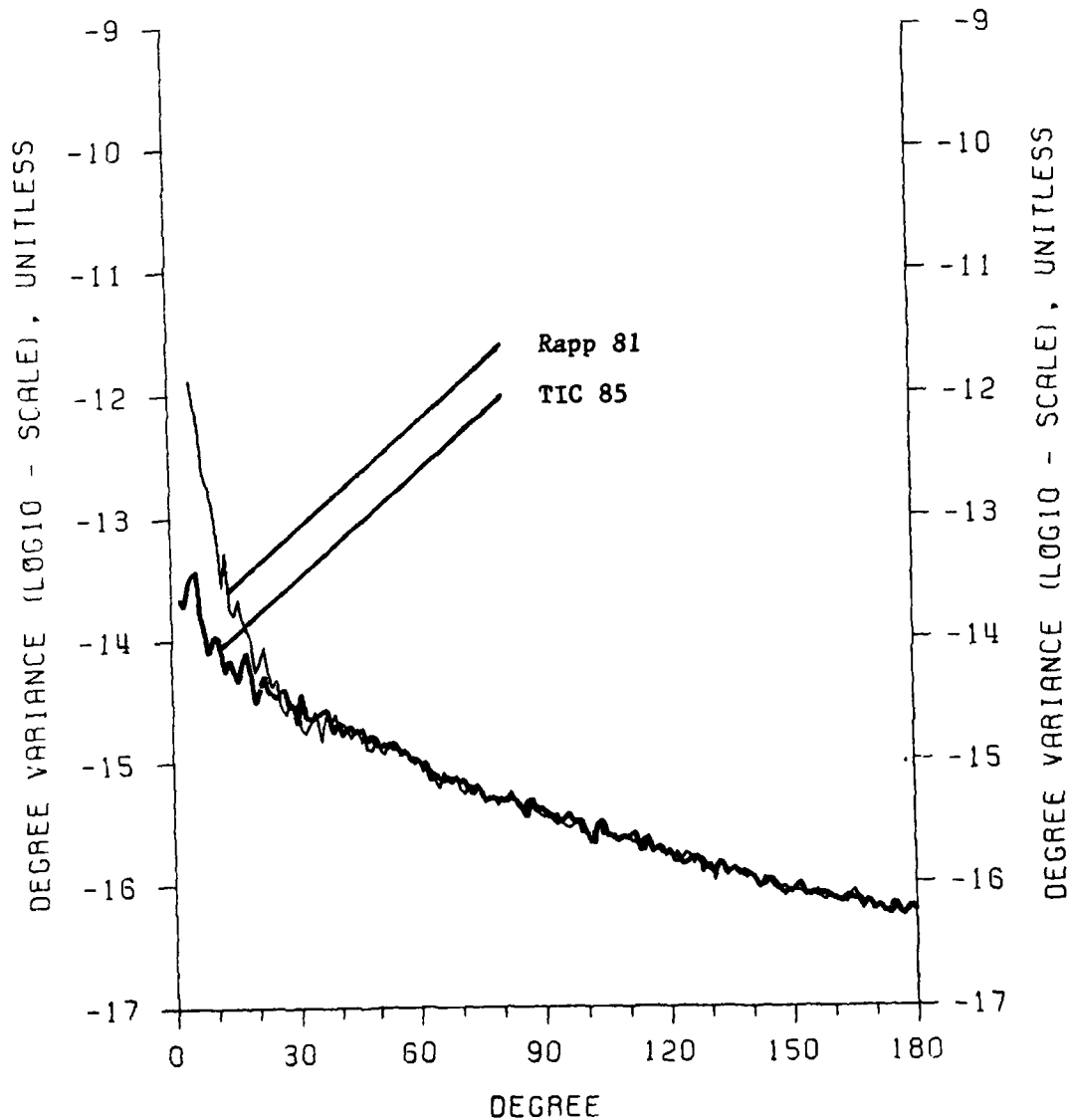


Fig. 6.6 Rapp 81 and optimal Airy/Vening Meinesz degree variances

The compensation smoothing $\bar{H}' = B * \bar{H}'$ was naturally performed in the frequency domain. The higher powers of \bar{H}' could have been obtained by spectral convolution in the frequency domain. We found it a lot easier to retransform the spectrum \bar{H}'_{nm} into the space domain using Colombo's Fourier synthesis program SSYNTH and to calculate all powers of \bar{H}' there. The binomial expansion has been terminated at power $j = 5$. After two iterations of the least-squares parameter estimation process no significant change of D and b could be observed. The finally adopted compensation model parameters, which yield a best possible agreement between gravity field information and a topography-isostasy implied model gravity field on a global scale, were

$D = 24 \text{ km}$ $b = 0.0091$

(6-2)

with a standard deviation of less than 2% (!) each. Note that the very low frequency part of $n < 15$ has been excluded from the parameter estimation process in order to avoid a strong bias of the solution coming from that part of the power spectrum which has the least to do with isostasy. The "best" smoothing operator $B(\psi)$ with $b = 0.0091$, normalized to $B(0) = 1$, is presented in Fig. 6.5 as a function of the spherical distance ψ . Finally we present in Fig. 6.6 both the power spectrum of the Rapp 81 geopotential solution and the power spectrum implied by the "best" Airy/Heiskanen-Vening Meinesz topographic-isostatic model. Because of the above-mentioned exclusion of the very low frequency part a match in that range can never be expected (and if observed, is purely artificial). The very long wavelengths, corresponding to that very low frequency part, are to a great extent due to density disturbances in the earth's mantle and are only superimposed by a relative little topographic-isostatic effect. Therefore, we should primarily focus on the higher and highest frequencies. And indeed, in this range the agreement of the two spectra is not only remarkable - it is almost unbelievable. At least from degree 36 on the match is very good and, as we believe, a considerable improvement compared with earlier solutions (compare Rapp, 1982).

The compensation smoothing due to Vening Meinesz yields not only a better agreement with observed reality, it also makes Forsberg's argument of

anticroots with tops partly above the ocean bottom, a phenomenon observed with the conventional Airy/Heiskanen model, obsolete because the compensation smoothing largely eliminates those singularities. An argument in favor of a smaller compensation depth is the observed thickness of the crust below the oceans which is of the order of 6-8 km; our model is in good agreement also with this figure. Another argument which speaks in favor of a Vening Meinesz model and against the simple Airy/Heiskanen model is the fact that the strength of the earth's crust is able to support a certain amount of topographical load without local yielding, while in the 1:1 model of Airy/Heiskanen free mobility between vertical mass columns is presupposed - a highly unlikely case. It remains an interesting exercise of applied elasticity theory to figure out whether the Gaussian compensation smoothing with the parameter $b = 0.0091$, estimated from global geodetic evidence only, is compatible with the known elastic parameters of the crust. Geophysicists are also invited to comment on our geodetic estimate of the depth of compensation. In any case, we should carefully keep in mind that our model is a global one with only two parameters - it can hardly be simpler. Therefore, it must be considered as a model describing the average behavior of the crust on a global scale. Local deviations from this global model, even large ones, are possible and are well-known from geophysical/geological evidence to exist. Therefore, this model can never be adequate to describe or even explain density patterns which are due to plate tectonics, like slabs sliding down into the mantle at plate margins or the like. Needless to say, this was not the goal of our investigation.

Geodesists have been and are still using the concept of isostasy for filtering purposes only, without bothering very much about its geophysical significance. They are happy with any isostatic model as long as the power of their measured gravity field signal is sufficiently diminished; as long as the topographic-isotatically reduced gravity field signal is sufficiently smooth, geodesists can live with that model. The Vening Meinesz model proposed here is probably not capable of smoothing gravity field signals significantly better than conventional models which have been successfully used in the past, although numerical studies in geodetically pathological areas along trenches and continental margins suggest more optimism. The model presented here should be understood as a bridge between geodesy and geophysics, which is

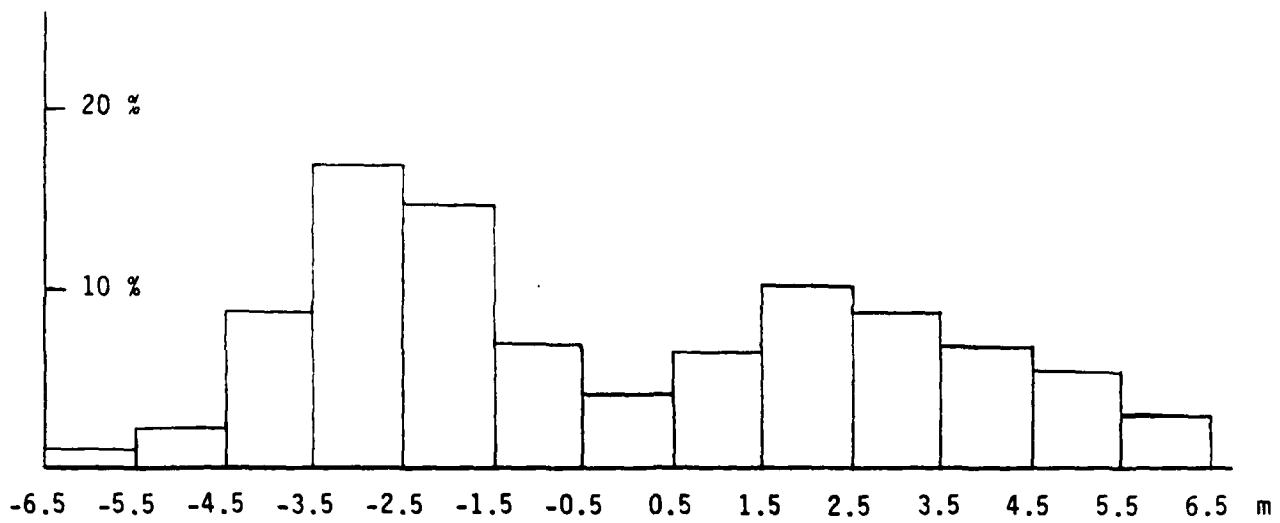


Fig. 6.7 Histogram of TIC 85 geoidal heights

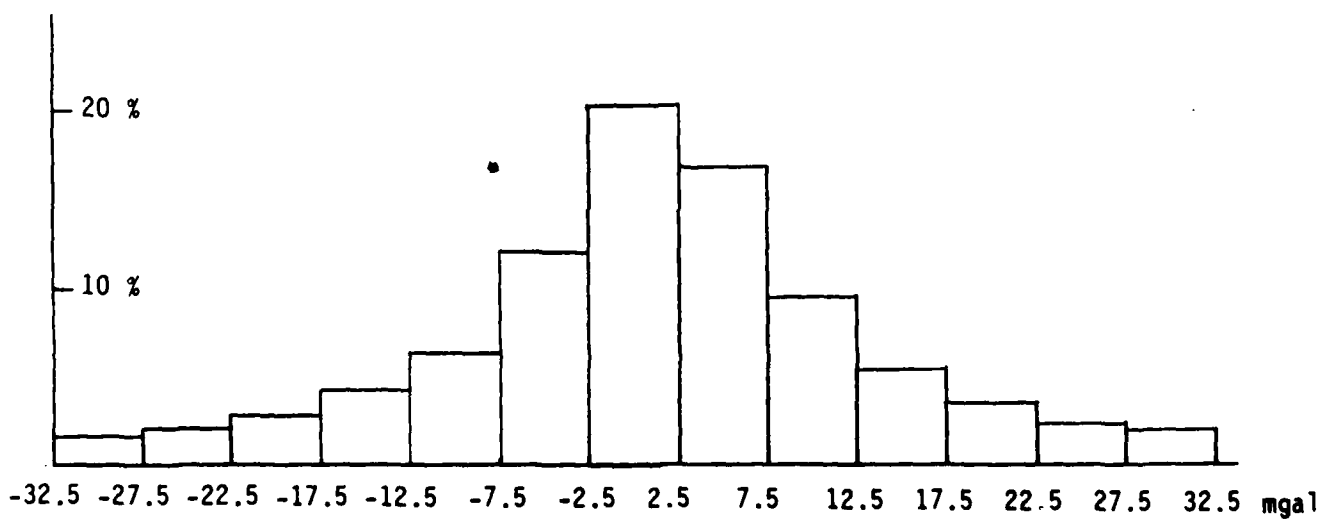


Fig. 6.8 Histogram of TIC gravity anomalies

more stable and sound than the ones that have been used by geodesists in the past. It is a model which makes us cheat less and therefore, enables us to live scientifically more comfortably.

The harmonic coefficients of the topographic-isostatic potential (called TIC 85), which are based on the model parameters (6-2) and derived from the DMAAC DTM dataset, have been synthesized using Colombo's Fourier algorithm SSYNTH, yielding both topographic-isostatic geoidal heights and gravity anomalies on a global $1^\circ \times 1^\circ$ grid.

The minimum and maximum geoidal height implied by TIC 85 are -10 m and $+30$ m with a variance of 17 m^2 which, compared to the observed value of about 900 m^2 , clearly demonstrates the strong power of non-isostatic effects due to deep density sources which is also reflected by the pronounced disagreement between the TIC 85 and the Rapp 81 solution in the very low frequency range. It is instructive to compare the minimum and maximum TIC 85 geoidal heights with those derived from the rule of thumb formula (which does not presuppose compensation smoothing) of equation (3-17): with the minimum and maximum DTM terrain heights of -7800 m and $+5900$ m equation (3-17) yields estimates of -12 m and $+25$ m which differ by only 20% from what we have obtained. (It is also interesting to note that the compensation smoothing reduces the root/antiroot maxima by about 30%.) The histogram of TIC 85 geoidal heights which is presented in Fig. 6.7 documents basically the distribution of rock (+) and ocean (-) masses.

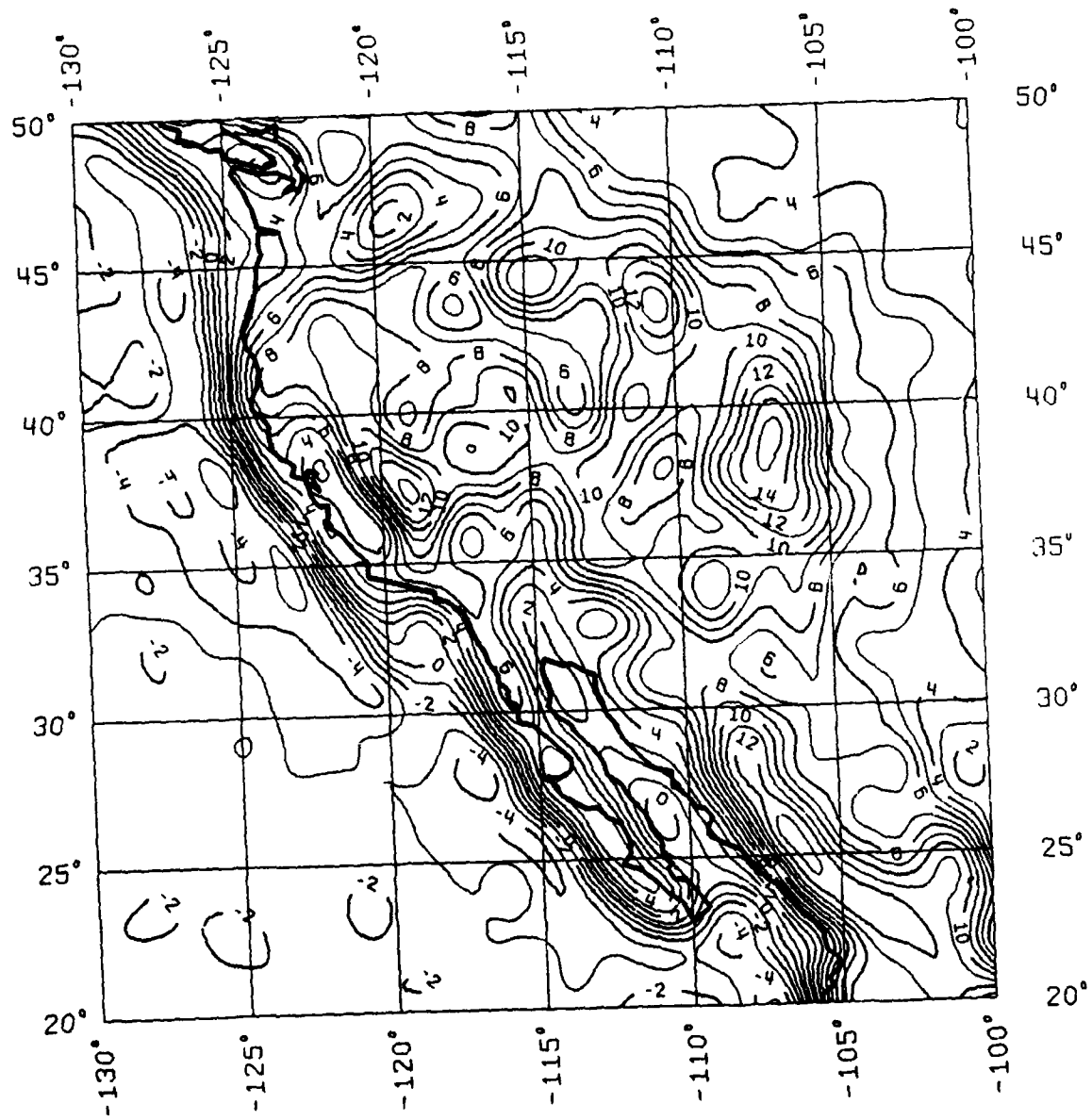
As far as TIC 85 implied gravity anomalies are concerned, we have minima and maxima of -225 mgal and 214 mgal with a variance of 516 $mgal^2$ which comes already much closer to the observed variance of $1^\circ \times 1^\circ$ mean gravity anomalies of about 900 $mgal^2$. This had to be expected because gravity responds much more to local density disturbances than the potential. The histogram of TIC 85 gravity anomalies in Fig. 6.8 has a pronounced maximum at zero and is almost symmetrically bell-shaped.

From these simple but instructive statistical data we can already anticipate the main features of the topographic-isostatic geoid: it mirrors topography to a

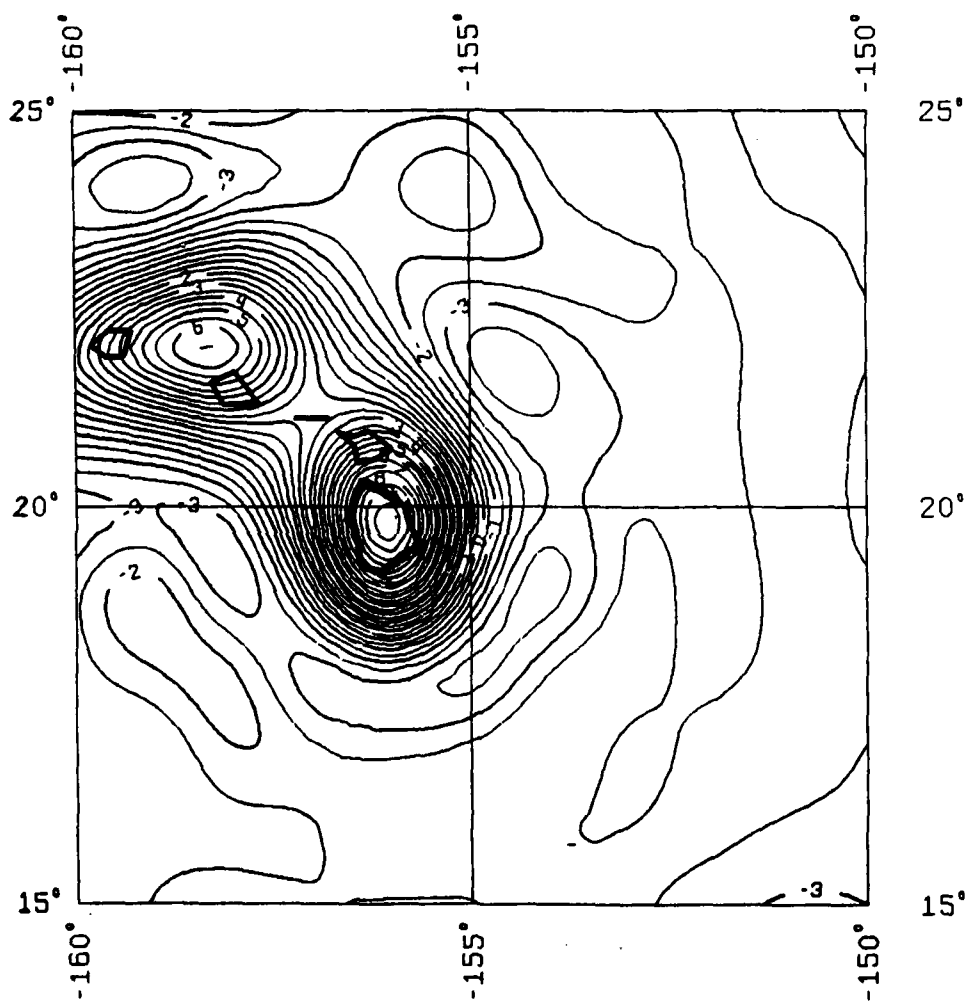
great extent and does hardly resemble the observed geoid on a global scale because of the missing long wavelength information. However, locally the TIC geoid comes very close to the observed trend-reduced geoid. Geoid maps, produced by GSPP (Sünkel, 1980) for various geodetically challenging "hot spots" on our earth are provided as illustration material. The reader is invited to make a comparison with the SEASAT - geoid derived by Rapp (1982b) and with the topographic-isostatic geoid, based on Airy/Heiskanen models of various depths and using the much more detailed and accurate SYNAPS bathymetric dataset (5' x 5' compared with the 1' x 1' DMAAC model), calculated by Forsberg (1984) for some pleasant resort areas on our globe.

The TIC 85 model got input from a worldwide DTM with a maximum resolution of about 200 km wavelength and very poor performance in some identified areas like South Africa, for example. Because our operators are well-known to be gigo's (garbage in-garbage out), we strongly suggest to improve the global DTM both with respect to resolution and accuracy in order to make a computation of an even better model up to degree and order 360 possible. Topographic-isostatic models of that high resolution are not only important for geophysical research, they are also extremely useful for the topographic-isostatic reduction of geodetic data: using a high resolution model like TIC 85 or better as a global reference, the entire topographic-isostatic reduction problem can practically be reduced to the processing of small residuals in planar approximation. And for that purpose we have again the very powerful FFT algorithm at our disposal which has been so successfully applied by Sideris (1984) for the evaluation of DTM-related integrals, or alternatively, the recently published TC-programs written by Forsberg(1984).

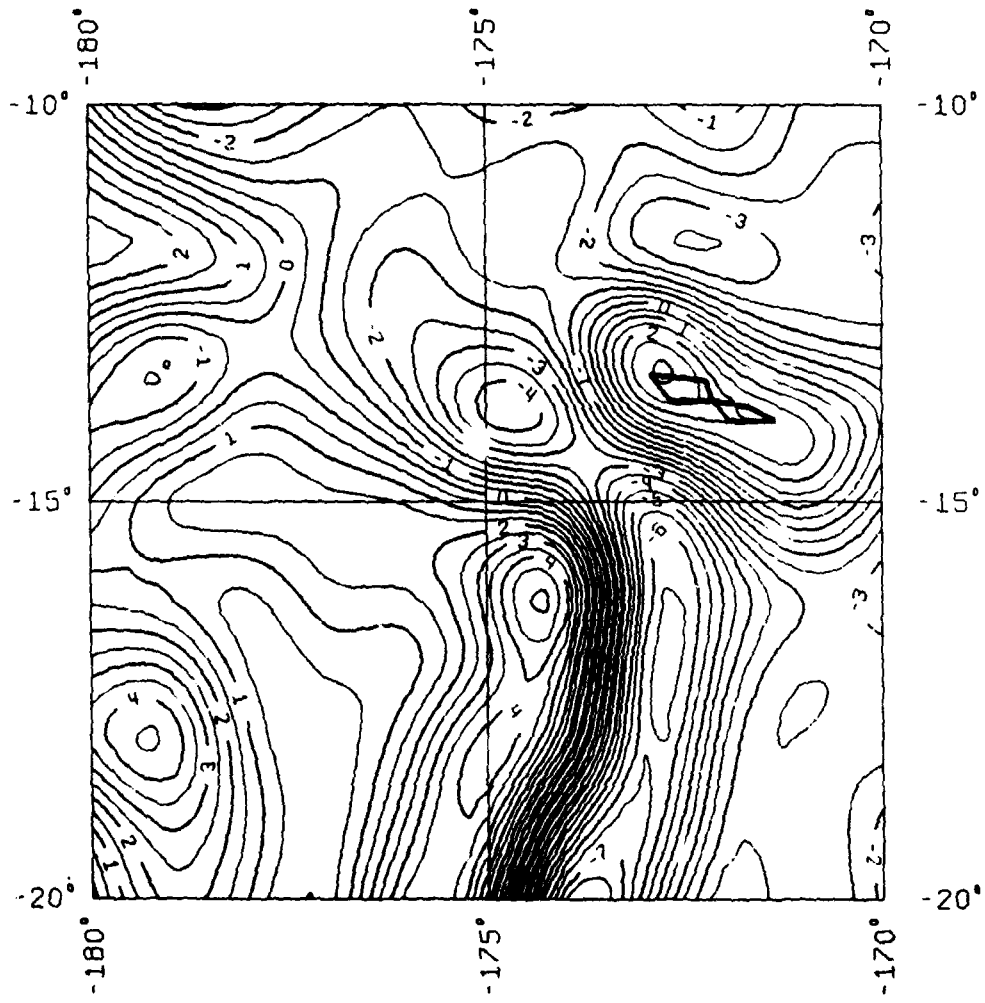
We consider this report (which claims neither to be complete nor to be completely debugged, despite the heavy use of a scientific word processing system) as a small step towards a better understanding of our earth's shell, which A. Wegener once compared to a defendant who declines to answer. The earth scientist, confronted with that defendant, is the judge who has to find the truth from the circumstantial evidences.



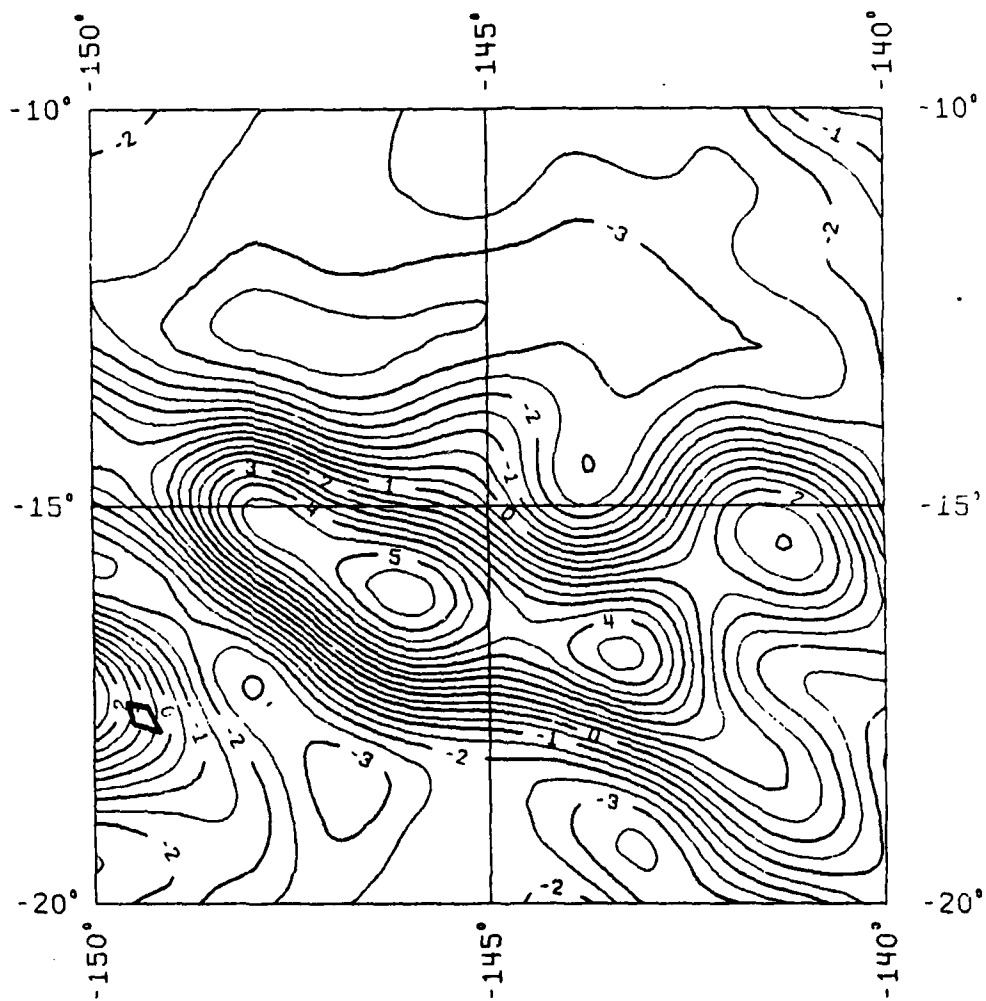
Map 1 TIC 85 geoid
USA/West Coast



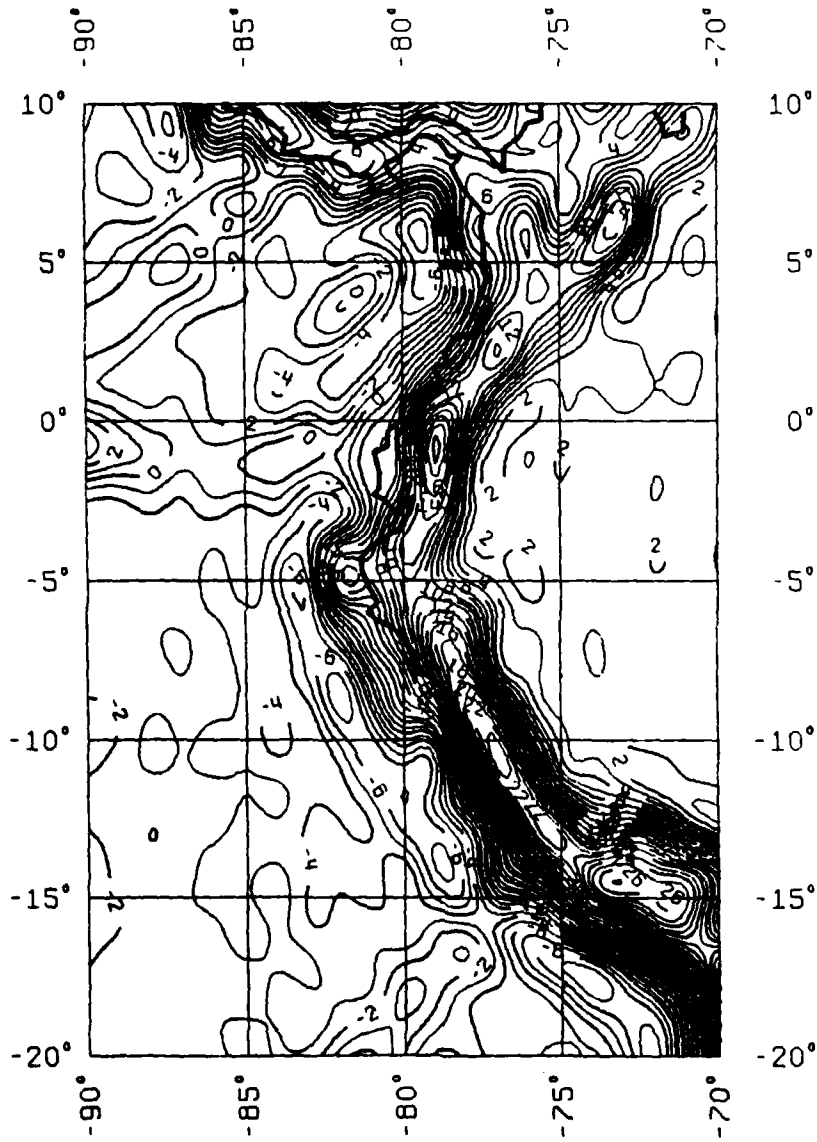
Map 2 TIC 85 geoid
USA/Hawaii



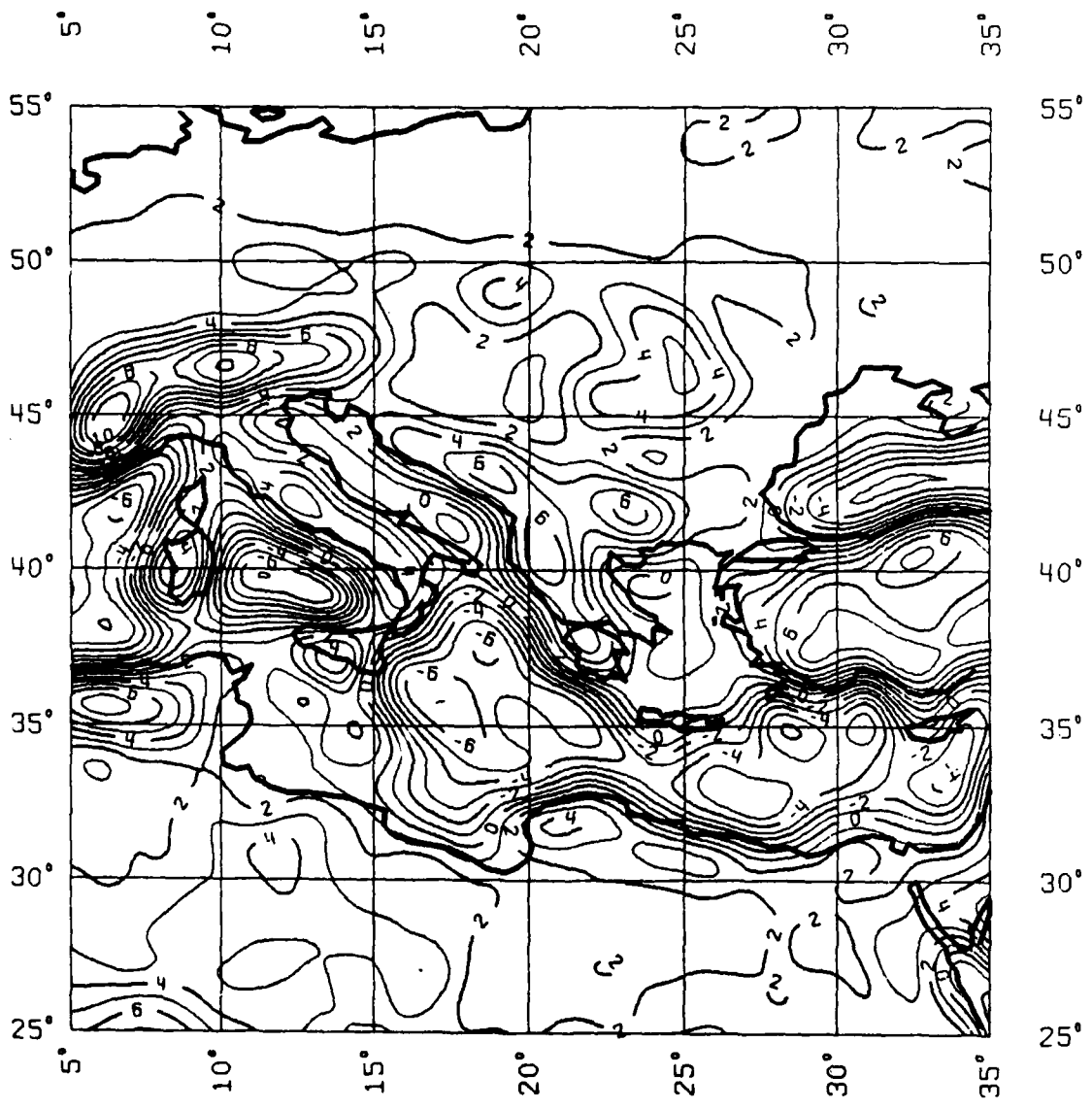
Map 3 TIC 85 geoid
Tonga Trench



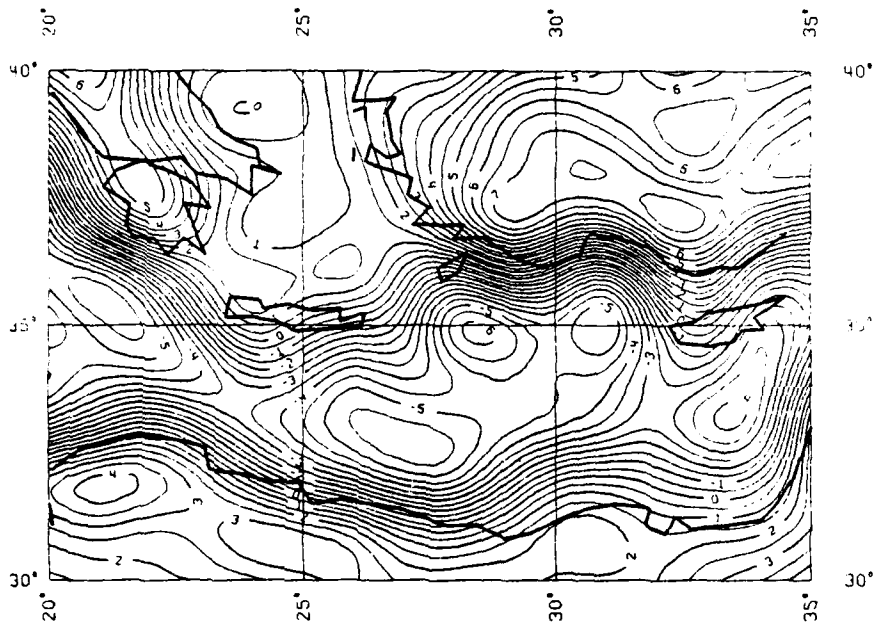
Map 4 TIC 85 geoid
Tahiti



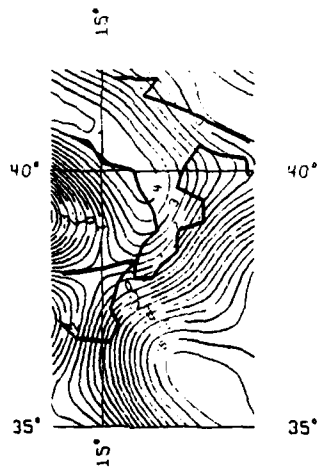
Map 5 TIC 85 geoid
South America/West Coast



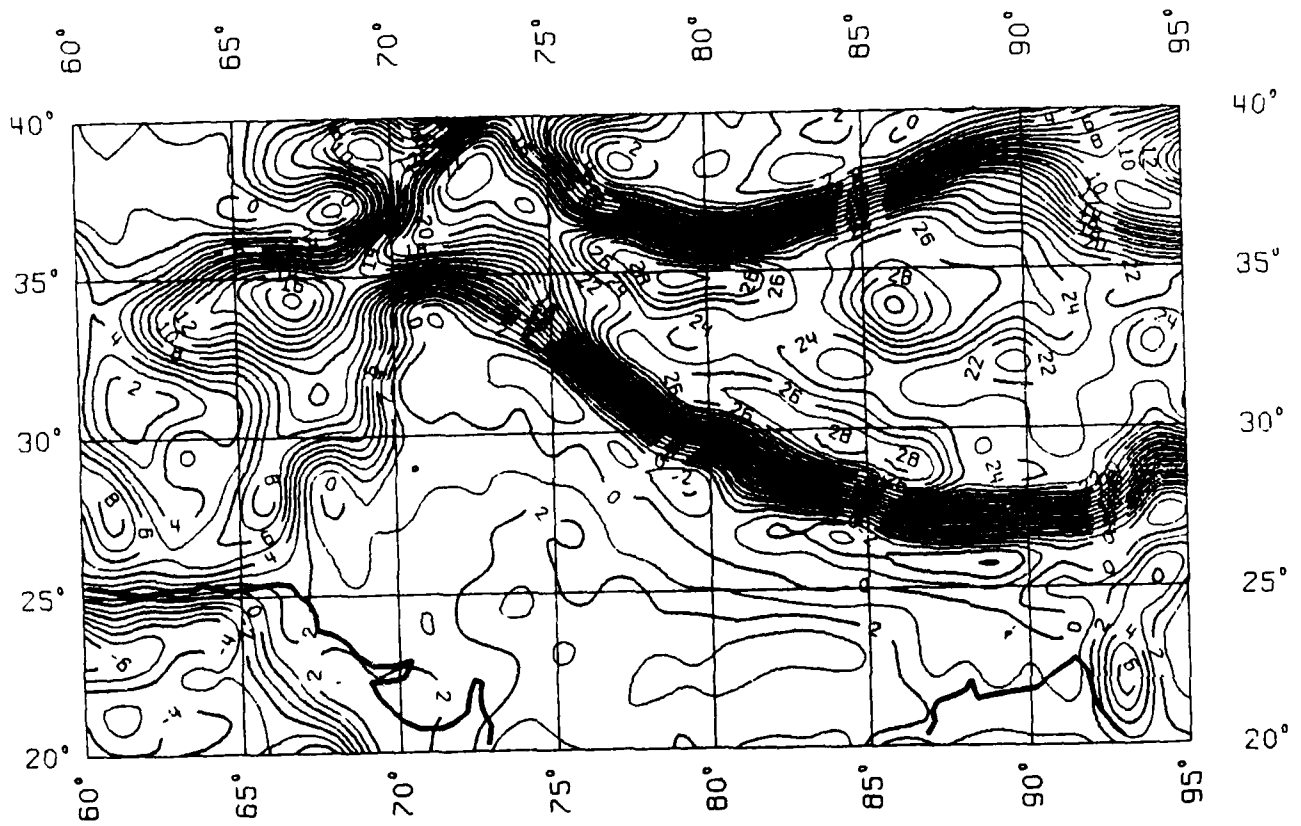
**Map 6 TIC 85 geoid
Mediterranean area**



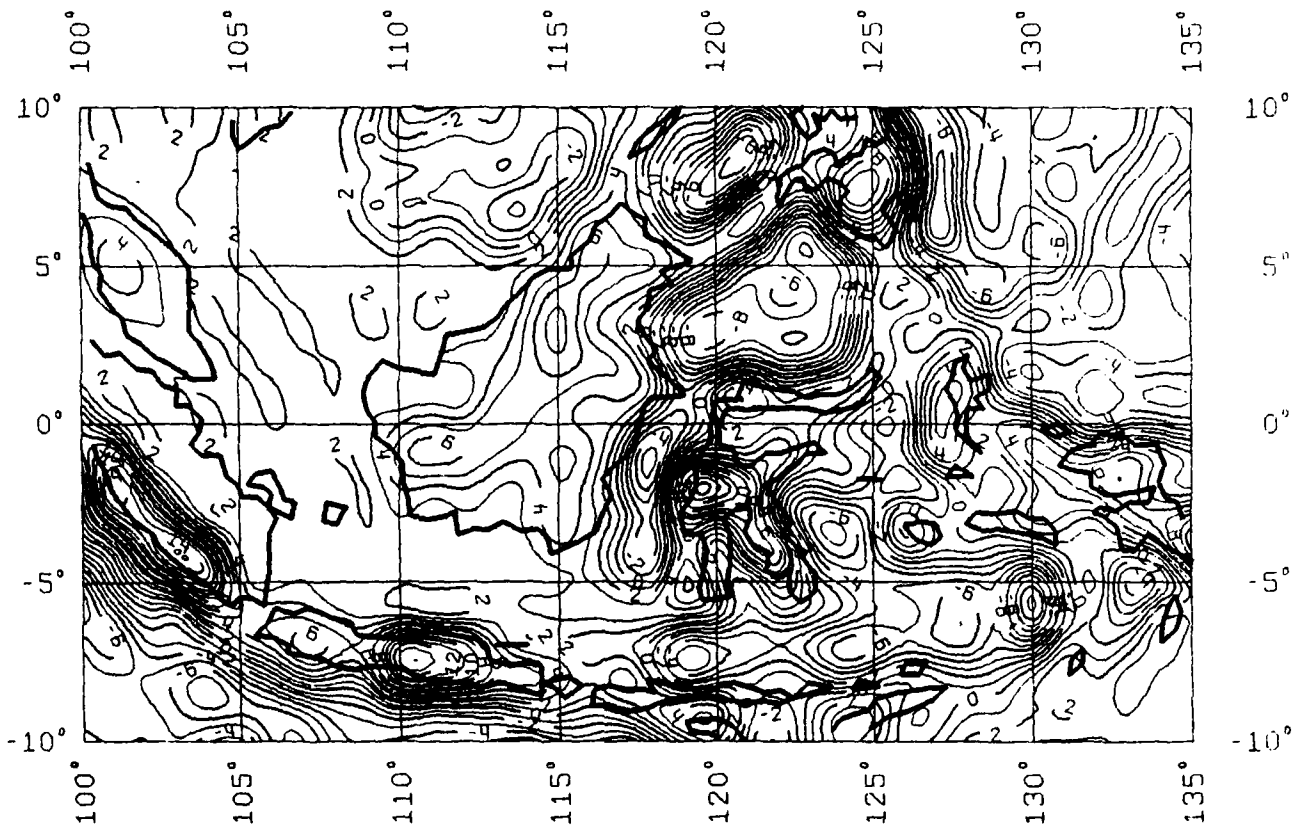
Map 7 TIC 85 geoid
Greece



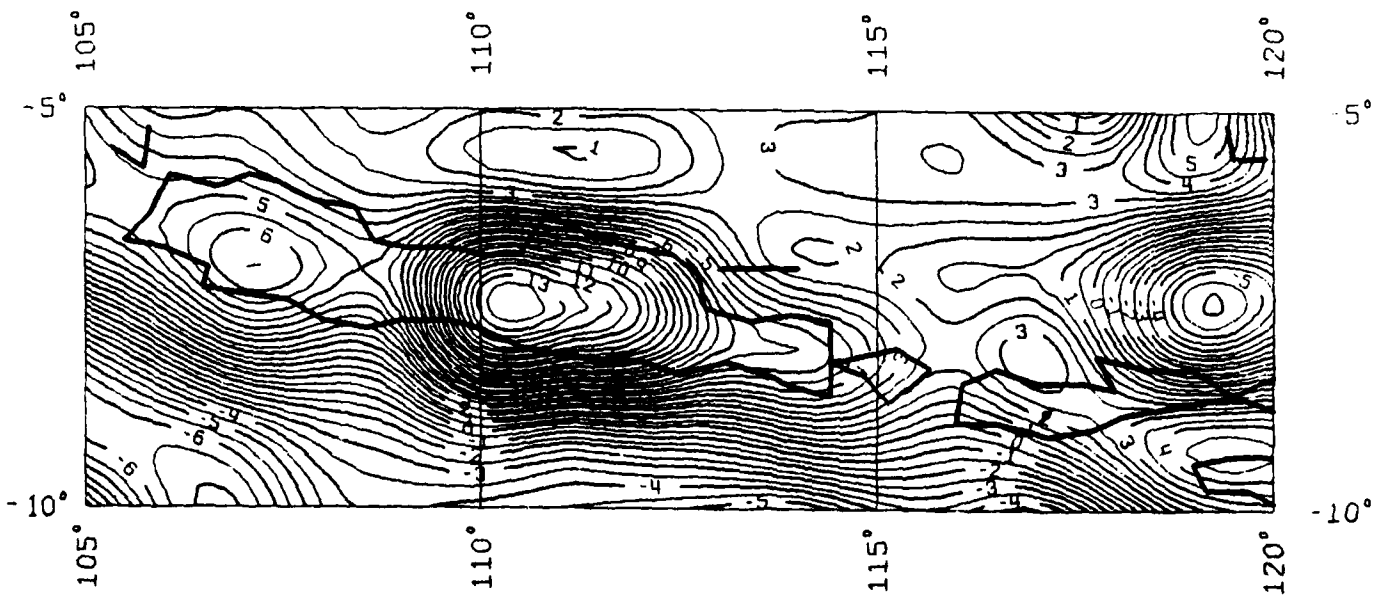
Map 8 TIC 85 geoid
Italy/Sicily



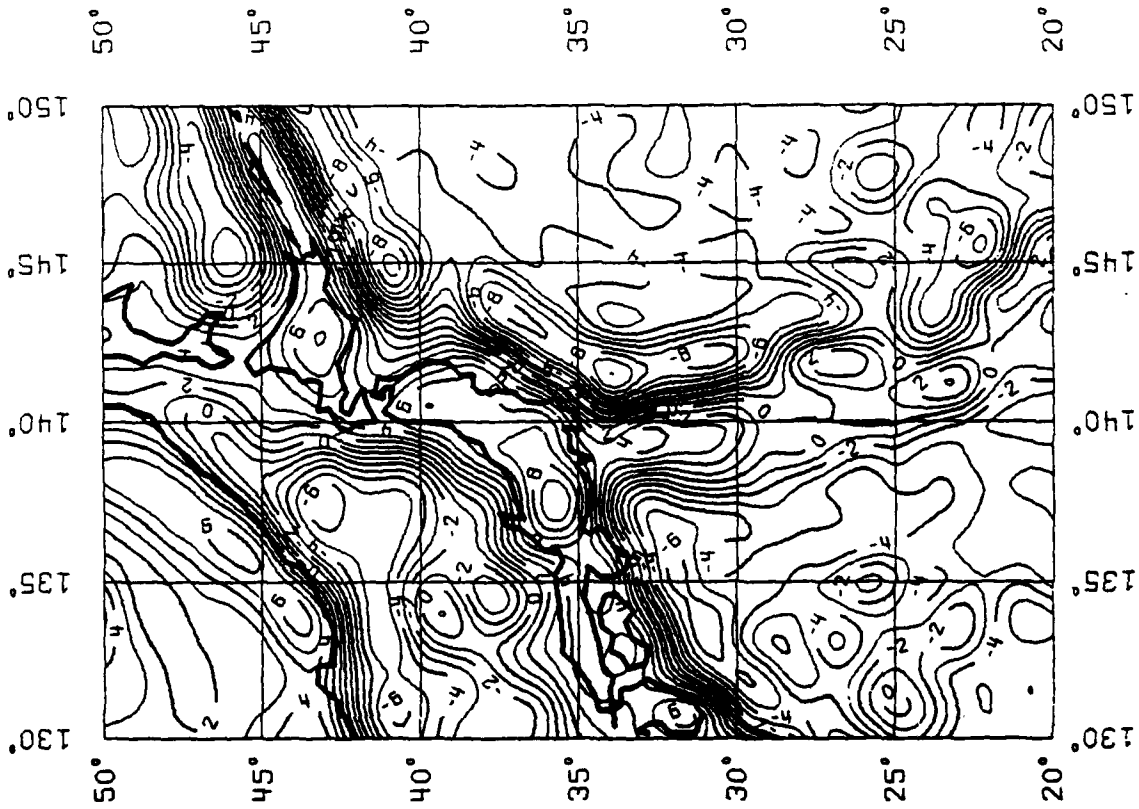
Map 9 TIC 85 geoid
Asia/Tibet



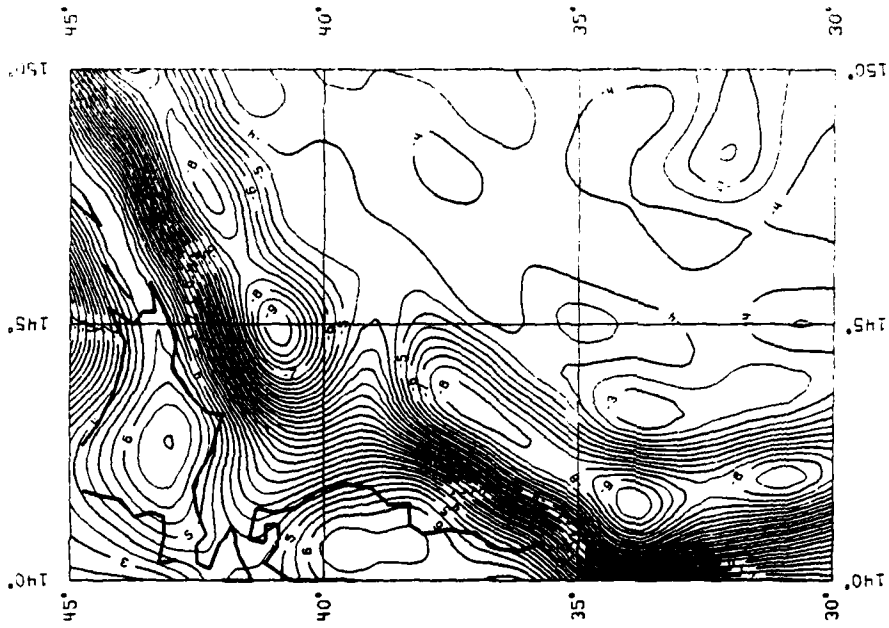
Map 10 TIC 85 geoid
Indonesia



Map 11 TIC 85 geoid
Java/Bali



Map 12 TIC 85 geoid
Japan



ACKNOWLEDGEMENTS

The author wishes to thank the project supervisor Prof. Dr. U.A. Uotila for both his scientific and administrative support, Prof. Dr. R.H. Rapp for valuable discussions and for providing unlimited access to the program library of the Department of Geodetic Science and Surveying. Thanks also to the young(er) fellows at the Department; without their advice many long nights at the computer would have been even longer. Special thanks go to Karen Wasielewski for her competent use of the scientific word processing system.

Computer time on the IBM 3081 system has been made available by the Instruction and Research Computer Center at the Ohio State University.

REFERENCES

- Colombo, O.L. (1981): Numerical methods for harmonic analysis on the sphere. AFGL-TR-81-0038, AD-A104-178.
- Forsberg, R. (1984): A study of terrain reductions, density anomalies and geophysical inversion methods in gravity field modelling. AFGL-TR-84-0174, AD-A150-788.
- Heiskanen, W.A. and H. Moritz (1967): Physical Geodesy. Freeman, San Francisco.
- Jekeli, Ch. (1979): Global accuracy estimates of point and mean undulation differences obtained from gravity disturbances, gravity anomalies and potential coefficients. OSU Report No. 288, Columbus, Ohio.
- Khan, M.A. (1973): Earth's isostatic gravity anomaly field. GSFC, Document No. X-592-73-199, Greenbelt, MD.
- Lachapelle, G. (1975): Determination of the geoid using heterogeneous data. Mitteilungen der geodätischen Institute der Technischen Universität Graz, Folge 19.
- Lambeck, K. (1979): Methods and geophysical applications of satellite geodesy. Rep. Prog. Phys. 42, pp. 547-628.
- Moritz, H. (1968): On the use of the terrain correction in solving Molodensky's problem. AFCRL-68-0298, AD-676-302.
- Moritz, H. (1980): Advanced Physical Geodesy. Wichmann-Verlag, Karlsruhe.
- Rapp, R.H. (1982a): Degree variances of the earth's potential, topography and its isostatic compensation. Bull. Géod., No. 56, pp. 84-94)

Rapp, R.H. (1982b): A global atlas of sea surface heights based on the adjusted SEASAT altimeter data. OSU Report No. 333, Columbus, Ohio.

Schwarz, K.-P. (1976): Geodetic accuracies obtainable from measurements of first and second order gravitational gradients. AFGL-TR-76-0189, AD-A031-331-2GA.

Sideris, M. (1984): Computation of gravimetric terrain corrections using fast Fourier transform techniques. Publication No. 20007, Division of Surveying Engineering, The University of Calgary, Alberta.

Sünkel, H. (1980): A general surface representation module designed for geodesy. AFGL-TR-80-0204, AD-A092-918.

Tscherning, C.C. (1985): On the long-wavelength correlation between gravity and topography. Proceedings of the 5th International Symposium "Geodesy and Physics of the Earth", Part II, pp. 134-142, Magdeburg, GDR, Sept. 23-29, 1984. Veröffentlichungen des Zentralinstituts für Physik der Erde, Nr. 81, Potsdam

Vening Meinez, F.A. (1939): Tables Fundamentales pour la réduction isostatique régionale. Bull. Géod., No. 63, pp. 771-776.

END

FILMED



DTIC